Continued exploration of 1,2,4-oxadiazole periphery for carbonic anhydrase-targeting primary arene sulfonamides: discovery of subnanomolar inhibitors of membrane-bound *h*CA IX isoform that selectively kill cancer cells in hypoxic environment

Mikhail Krasavin[a,*], Anton Shetnev[b], Tatyana Sharonova[a], Sergey Baykov[a], Stanislav Kalinin[a], Alessio Nocentini[c], Vladimir Sharoyko[a], Giulio Poli[d], Tiziano Tuccinardi[d], Sofia Presnukhina[b], Tatiana B. Tennikova[a], Claudiu T. Supuran[c,*]

[a] Saint Petersburg State University, Saint Petersburg, 199034 Russian Federation

[b] The Ushinsky Yaroslavl State Pedagogical University, Yaroslavl 150000, Russian Federation

[c] Neurofarba Department, Universita degli Studi di Firenze, Florence, Italy

[d] Department of Pharmacy, University of Pisa, 56126 Pisa, Italy

* Corresponding authors. E-mail addresses: m.krasavin@spbu.ru (M. Krasavin), claudiu.supuran@unifi.it (C. T. Supuran)

ABSTRACT

An expanded set of diversely substituted 1,2,4-oxadiazole-containing primary aromatic sulfonamides was synthesized and tested for inhibition of human carbonic anhydrase I, II, IX and XII isoforms. The initial biochemical profiling revealed a significantly more potent inhibition of cancer-related membrane-bound isoform *h*CA IX (reaching into submicromolar range), on top of potent inhibition of *h*CA XII, that is another cancer target. The observed structure-activity relationships have been rationalized by molecular modeling. Comparative single-concentration profiling of the carbonic anhydrase inhibitors synthesized for antiproliferative effects against normal (ARPE-19) and cancer (PANC-1) cancer cell lines under chemically induced hypoxia conditions revealed several candidate compounds selectively targeting cancer cells. More in-depth characterization of these leads revealed two structurally related compounds that showed promising selective cytotoxicity against pancreatic (PANC-1) and melanoma (SK-MEL-2) cell lines.

Keywords: carbonic anhydrase; isoform-selective inhibitors; periphery groups; primary sulfonamides; subnanomolar inhibition; 1,2,4-oxadiazole; isosteric replacement; cancer cells; hypoxic environment.

1. Introduction

Human carbonic anhydrases (*h*CAs) catalyze a simple, yet fundamental biochemical reaction of reversible hydration of carbon dioxide [1]. This reaction produces bicarbonate anion and a proton and thus is central to regulating pH inside and outside the cells in various tissues and organs. There are 15 enzymes in humans which are carbonic anhydrases and they differ in cellular localization, catalytic activity and expression levels between normal and disease states [2]. Various *h*CA isoforms continue to be validated as targets for novel disease treatment [3]. Targeting of bacteria via selective inhibition of CAs that are vital to pathogen without affecting those of the human host is a novel platform for the development of future antibiotics [4]. This makes carbonic anhydrases attractive as drug targets and mandates that small molecules designed to produce desired therapeutic effect are isoform-selective so as not to affect the normal functioning of other isoforms, not involved in the onset of the disease. Today, however, virtually all clinically used carbonic anhydrase inhibitors (such as diuretics [5] or treatments for glaucoma-related intraocular hypertension [6]) are non-selective inhibitors exerting their therapeutic effect via inhibition of *h*CA II isoform as illustrated by the drugs in Fig. 1.

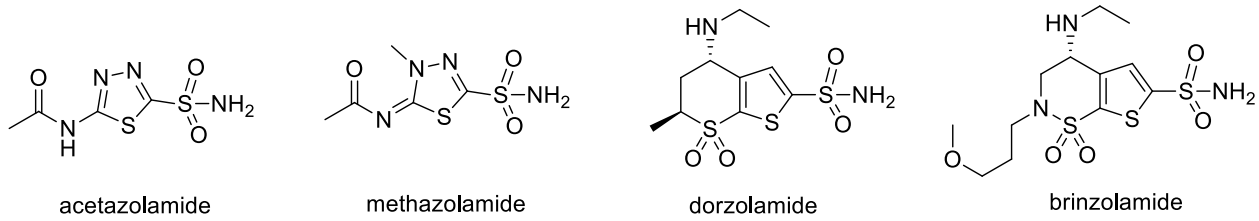

Fig. 1. Examples of clinically used, non-selective *h*CA inhibitors.

The situation with non-selectivity of carbonic anhydrase inhibitors (CAIs) investigated as potential drugs has been improving as is evidenced by the emergence of literature reports on highly isoform selective CAIs. Illustrative examples include isoxazole bis-sulfonamide inhibitor of membrane-bound *h*CA IV (**1**) [7], dual inhibitor of cytosolic *h*CA II and VII based on 2-imidazoline scaffold (**2**) [8], selective biphenyl sulfonamide inhibitor of *h*CA XIV (**3**) [9], and ring-opened *N*-alkyl saccharin derivative (**4**) selective for tumor-associated, membrane-bound isoforms hCA IX and XII [10]. In addition to these novel, discovery-phase CAIs, the most advanced investigational CAIs (also distinctly relevant to the results and context of present work) are compounds SLC-0111 and E7070 (Fig. 2).

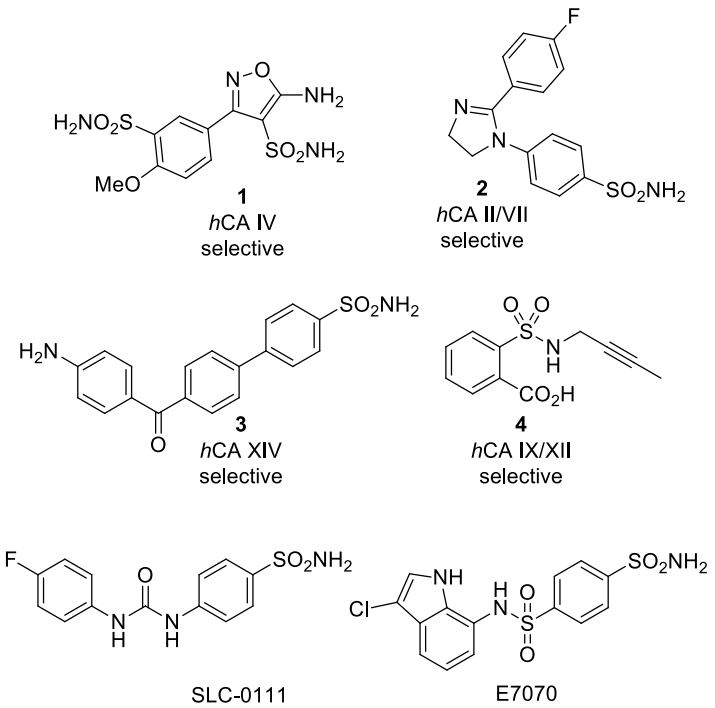

Fig. 2. Examples of recently reported isoform-selective hCA inhibitors (**1**-**4**) and structures of the most advanced *h*CA IX-selective (SLC-0111) and *h*CA IX/XII-selective (E7070) CAIs currently in clinical trials for cancer.

SLC-0111 has a marked selectivity toward *h*CA IX and has now successfully completed phase I clinical trials for tumors overexpressing CA IX [11]. It is scheduled to advance into phase II clinical trials in the near future. E7070 (indisulam) has been developed as novel antineoplastic therapy by Eisai Co., Ltd. First published in 2001 [12], it entered clinical development in 2005 and is currently in phase II clinical trials in the US and Europe [13]. In addition to inhibiting *h*CA IX and XII (validated antitumor targets, *vide infra*), albeit non-selectively vs. cytosolic *h*CA I and II [14], E7070 inhibits cyclin-dependent kinases (CDKs) that are vital for cell division.

Overexpression of membrane-bound *h*CA IX and *h*CA XII in metastatic tumors is the principal mechanism of tumor cell survival under stressful, hypoxic conditions and acidic extracellular environment which surrounds the tumor and is damaging to normal cells [15]. Thus, selective inhibition of either or both of these isoforms can lead to retardation of tumor growth and, ultimately, reduction of tumor size [16]. Considering today's pressing issue of tumors developing resistance to various targeted small-molecule therapies [17], the fundamental character of the above mechanism of tumor survival and low likelihood of emerging resistance via mutation of relevant biomolecules, makes selective targeting of *h*CA IX and/or *h*CA XII a particularly attractive therapeutic approach [18].

An overwhelming majority of CAIs developed and characterized today are based on primary arene sulfonamides where the sulfonamide group acts as a zinc-binding motif responsible for anchoring to the active-site prosthetic metal ion [19]. The main source of affinity toward carbonic anhydrases in general and selectivity toward a particular isoform are, consequently, additional interactions between the inhibitor's periphery and the protein surroundings of the active site where two distinct halves, a hydrophobic and a hydrophilic one, can be delineated [20]. While it is difficult to target a particular isoform based solely on *in silico* modeling, structural peculiarity of the carbonic anhydrase active site topology provides certain freedom in designing and screening novel chemical series to provide so-called 'seed SAR' (or initial structure-activity relationship information) which can be later capitalized upon via point-by-point medicinal chemistry optimization of the compounds which have already displayed promising isoform inhibition profiles.

In the course of exploring various substituted heterocyclic appendages for the CAI pharmacophoric arene sulfonamide moiety (such as 1,3-oxazole [21], isoxazole [7], imidazoline [8], pyrazole [22]), we discovered a promising class of CAIs, namely, 1,2,-oxadiazol-5-yl benzene sulfonamides **5** which displayed, in addition to potent inhibition of *h*CA II (a typical off-target of arene sulfonamides), a low-nanomolar inhibitory properties toward *h*CA IX (as illustrated by representative compound **5a** [23]). Encouraged by this finding and mindful of the importance of continuous discovery of novel CA IX inhibitors to feed into anticancer development pipeline, we continued exploring structure-activity relationships based on the 'seed SAR' set [23] and aimed to: i. replace the *p*- and *m*-phenylene linker with 3,5-thienylene (**7**), ii. perform an isosteric swap of R group and aminosulfonyl(hetero)aryl moiety by exploring 1,2,4-oxadiazol-3-yl arene sulfonamides **8**, iii. evaluate the inhibitory profile of series **7** and **8** against a panel of *h*CA isoforms (including *h*CA IX and *h*CA XII) and iv. validate the mechanism-based utility of promising *h*CA IX and/or *h*CA XII inhibitors for selective targeting cancer cells under hypoxic conditions. Herein, we summarize the results of these studies.

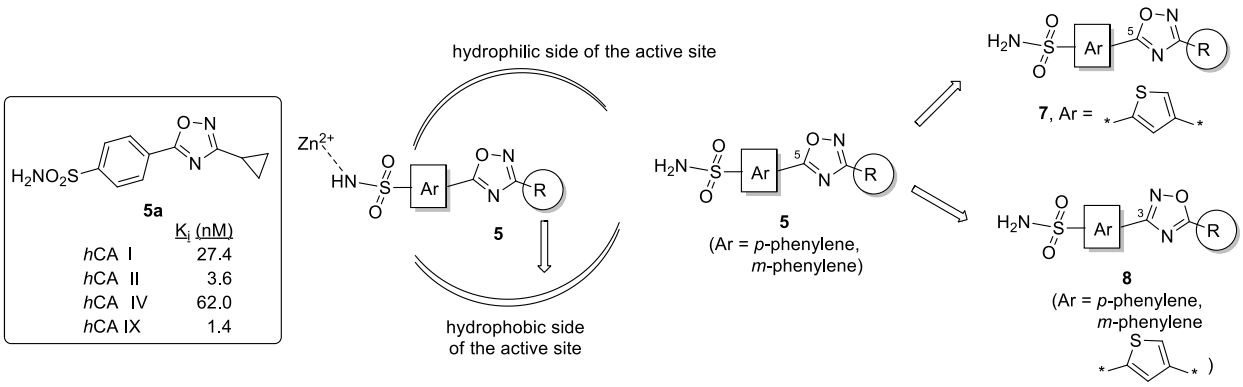

Fig. 3. Earlier reported 1,2,4-oxadiazol-5-yl benzenesulfonamides **5** (their design rationale and representative compound (**5a**) CAI profile) and SAR exploration plan (**5** → **7** and **8**) implemented in this work.

2. Results and discussion

2.1. Chemistry

In analogy to the previously described synthesis of compounds **5**, commercially available (albeit costly) 5-sulfamoylthiophene-3-carboxylic acid (**9**) was prepared on multigram scale by direct sulfochlorination of thiophene-3-carboxylic acid followed by reaction of the intermediate sulfonyl chloride with ammonium hydroxide solution in acetonitrile. Carboxylic acid **9** was activated as respective imidazolide by treatment of its solution in DMSO with CDI and was brought in contact with amidoximes **10a-e** which had been prepared from respective nitriles **11a-e** using the literature procedure [24]. After *O*-acylation of amidoximes was complete, solid NaOH was added, to form a superbase solution which promoted cyclodehydration of *O*-acylamidoxime intermediate **12** [25-28] and gave target compounds **7a-e** in good to excellent yields from **10a-e** (Scheme 1).

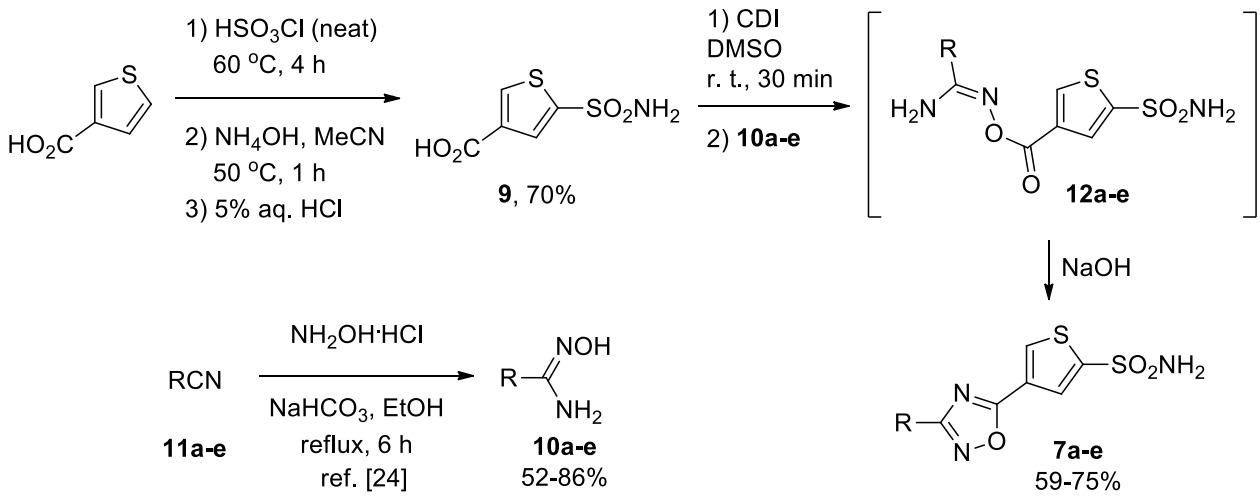

Scheme 1. Preparation of 4-(1,2,4-oxadiazol-5-yl)thiophene-2-sulfamides **7a-d**.

For the preparation of compounds belonging to the isomeric series (**8**), the pharmacophoric sulfamoyl group was to be integrated into the structure of amidoxime synthon. The respective phenylamidoximes **10f-h** (Ar = 4-$H_2NO_2SC_6H_4$, 3-$H_2NO_2SC_6H_4$ and 4-H_2NO_2S,2-$MeOC_6H_3$, respectively) were prepared directly from the corresponding nitriles **11f-h** according to the literature protocol [24]. These were acylated by either carboxylic acid methyl ester (RCO_2Me) or acyl imidazolide (RCO_2Im) in DMSO and cyclized into target 1,2,4-oxadiazoles **8a-p** on

treatment with superbase solution formed on addition of solid NaOH [25-28]. The corresponding 2-sulfamoylthiophene-4-carbonitrile starting material was found difficult to synthesize. Hence, the respective 1,2,4-oxadiazoles **8q-s** were prepared by an alternative route involving direct sulfochlorinatination of 3-(1,2,4-oxadiazol-3-yl)thiophenes **13a-c**. The latter were prepared from amidoxime **10g** via direct acylation-cyclization under superbasic conditions. (Scheme 2).

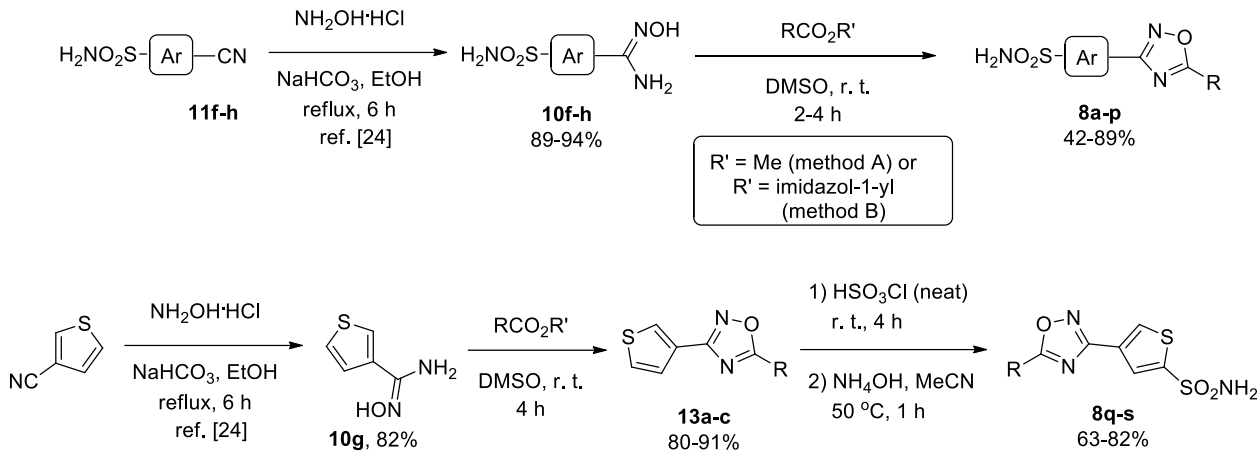

Scheme 2. Preparation of 1,2,4-oxadiazol-3-yl arenesulfamides **8a-s**.

2.2. Biochemical testing for CA inhibition

The twenty-four primary sulfonamide compounds **7a-e** and **8a-s** synthesized as detailed above, were tested in CO_2 hydration stopped-flow biochemical assay (see Experimental section) against two cytosolic (*h*CA I and II) and two membrane-bound, cancer-related *h*CA IX and XII isoforms to produce the inhibition data (K_i) summarized in Table 1.

Table 1. Inhibitory profile of compounds **7a-e** and **8a-s** against *h*CA I, II, IX and XII.[a]

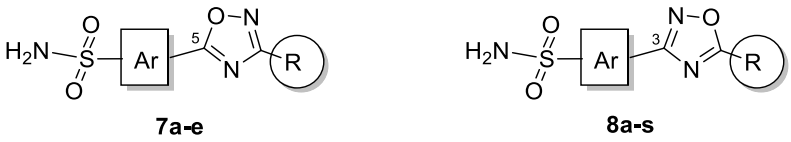

Compound	* — Ar — *	R	K_i (nM)			
			*h*CA I	*h*CA II	*h*CA IX	*h*CA XII
7a	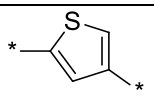	Ph	8.9	1.7	0.24	9.8
7b	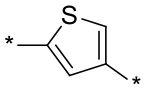	2-MeOC$_6$H$_4$	16.2	0.64	0.13	8.8

7c	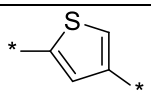		9.3	0.75	0.089	10.3
7d	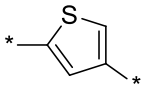	2-pyridyl	25.0	4.3	0.39	8.5
7e	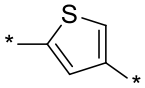	3-MeOC$_6$H$_4$	5.4	0.82	2.2	33.6
8a	*p*-phenylene		7.8	4.1	1.9	97.1
8b	*p*-phenylene	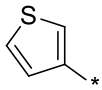	8.9	0.59	1.8	9.0
8c	*p*-phenylene	Ph	64.9	0.74	0.77	7.8
8d	*p*-phenylene	4-pyridyl	48.0	0.30	0.44	8.2
8e	*p*-phenylene	4-NCC$_6$H$_4$	88.2	0.44	0.60	8.5
8f	*p*-phenylene	2-pyridyl	37.5	0.93	0.31	9.5
8g	*p*-phenylene	3,4-diClC$_6$H$_3$	82.4	1.3	0.62	9.7
8h	*p*-phenylene	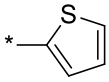	7.9	0.39	0.36	8.3
8i	*p*-phenylene	Me	37.9	0.48	0.53	8.6
8j	*m*-phenylene	Ph	343.9	20.8	3.7	8.3
8k	*m*-phenylene		758.5	8.9	92.4	8.9
8l	*m*-phenylene	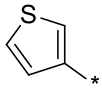	82.8	0.38	0.88	9.4
8m	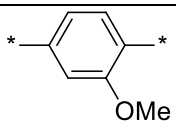	Ph	459.3	8.8	13.1	33.1
8n	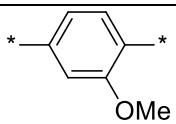	4-NCC$_6$H$_4$	779.4	593.1	273.8	32.9
8o	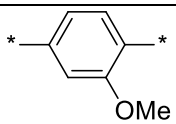	3-pyridyl	1024.1	270.5	12.1	16.8
8p	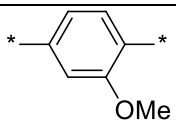	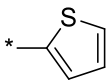	1163.3	92.1	15.9	32.1
8q	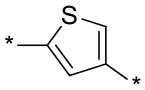	Me	8.1	0.91	1.6	10.1

8r	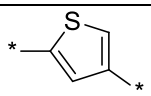		53.0	0.88	2.1	9.2
8s	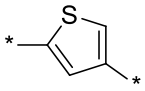	Ph	454.0	0.69	1.1	8.2
Acetazolamide			250.0	12.0	25.0	5.7

[a] Mean K_i values from 3 different stopped-flow assays (errors were in the range of 5-10% of the reported values).

From a brief examination of the data presented in Table 1, it becomes evident that in general, the compounds prepared and investigated in this work retained subnanomolar to low nanomolar inhibitory potency against cytosolic *h*CA II isoform while the potency toward cancer-related *h*CA IX now comfortably resides in the subnanomolar range, in contrast to previously reported 1,2,4-oxadiazole series **5** [23]. In addition to that, inhibition of the other membrane-bound isoform, *h*CA XII, inhibition of which has a similar potential for cancer treatment, was achieved with about 10 nM potency throughout (note that in this case, the SAR against *h*CA XII was surprisingly 'flat', i.e. insensitive to variation of the inhibitor structure). An obvious SAR trend evident from these data is the detrimental effect of the methoxy substituent in the phenylene linker (cf. compounds **8m-p**) on the inhibitory potency across the panel of the four isoforms interrogated. Particularly drastic is the observed drop in potency against *h*CA II for compound **8p** (in comparison to **8h**) and for compound **8n** (in comparison to **8e**). Interestingly, while **8p** retained much of the potency against *h*CA XII, **8n** did not. Compounds **7a-e** in general displayed a desirable trend to improved *h*CA IX potency and selectivity against off-target *h*CA II (although inhibition of the latter does not present a significant obstacle to antitumor efficacy as evidenced by the advanced status of compound E7070, *vide supra*). Particularly significant in the double-digit picomolar potency of compound **7c** against *h*CA IX which is in sharp contrast to ~3 orders of magnitude lower potency displayed by **8k** which has a similar topology. A significant effect on *h*CA IX potency was observed for 1,2,4-oxadiazol-3-yl benzene sulfonamide **8f** (K_i(*h*CA IX) 0.31 nM) in comparison to its earlier reported direct "scaffold-hopping" counterpart belonging to general structure **5** (compound **6{20}** in reference [23]: K_i(*h*CA IX) 22.4 nM), which constitutes ~2 orders of magnitude difference.

Altogether, by comparing compounds with similar periphery from the "scaffold-hopping" prospective (Table 2), one can appreciate that replacing a 1,2,4-oxadiazol-5-yl periphery (Scaffold A) with a similarly substituted 1,2,4-oxadiazol-3-yl periphery (Scaffold B) can lead to improvement of *h*CA IX potency. A similarly fortunate scaffold choice is 1,2,4-oxadiazol-5-yl

thiophene (Scaffold E) which delivered the most potent *h*CA IX inhibitor **7c**. In general, transferring periphery groups from *p*-phenylene-linked Scaffold A onto Scaffold E resulted in significant increase in inhibitory potency.

Table 2. Analysis of the previously observed [23] and newly established (this work) structure-activity relationships for selected CAIs in the 1,2,4-oxadiazol-3(5)-yl arenesulfonamide series from the "scaffold-hopping" prospective (*h*CA II and *h*CA IX).

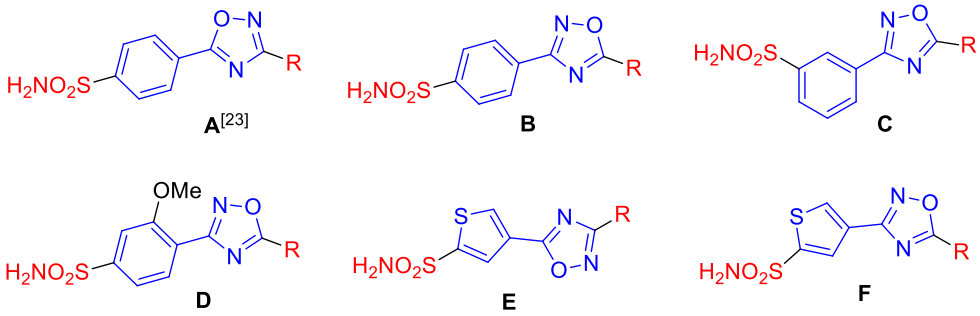

R↓	K_i (nM)											
	A[a]		B[b]		C[b]		D[b]		E[b]		F[b]	
	II	IX	II	IX	II	IX	II	IX	II	IX	II	IX
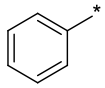	1.8	6.7	0.74	0.77	20.8	3.7	8.8	13.1	1.7	0.24	0.69	1.1
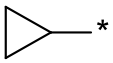	3.6	1.4	4.1	1.9	8.9	92.4	--	--	0.75	0.089	0.88	2.2
	44.3	1.6	0.39	0.36	--	--	92.1	15.9	--	--	--	--
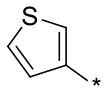	5.5	1.4	0.59	1.8	0.38	0.88	--	--	--	--	--	--
	0.72	22.4	0.93	0.31	--	--	--	--	4.3	0.39	--	--
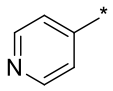	0.42	2.7	0.30	0.44	--	--	--	--	--	--	--	--
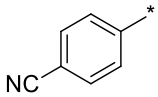	--	--	0.44	0.60	--	--	593.1	273.8	--	--	--	--
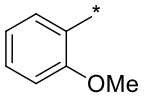	0.51	21.1	--	--	--	--	--	--	0.64	0.13	--	--
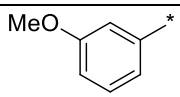	0.48	242.8	--	--	--	--	--	--	0.82	2.2	--	--

[a] Data reported in [23].

[b] Data from Table 1.

2.3. Antiproliferative activity against normal and cancer cell lines

The potent inhibition of membrane-bound, cancer-related enzyme *h*CA IX by virtually all compounds **7a-e** and **8a-s** (some of them reaching into the subnanomolar and even picomolar potency range), on top of fairly promising inhibition profile with respect to *h*CA XII, clearly warranted their further investigation for antiproliferative effects in cancer cells. It should be noted that the absence of selectivity between these isoforms and *h*CA II should not be perceived as a substantial disadvantage, considering the fact the vastly different cellular localization of these targets and, as a result, the potential for gaining selectivity by suppressing cell membrane permeability [29]. While evaluation of the antiproliferative profile for cancer cells in comparison to normal cells should be performed under normoxic as well as hypoxic conditions, sulfonamide CAs are known to more likely to exert their cytotoxicity profile under hypoxic conditions, i. e. those that closely reproduce the environment of a growing solid tumor, particularly with respect to pH disbalance and overexpression of *h*CA IX and *h*CA XII isoforms [30].

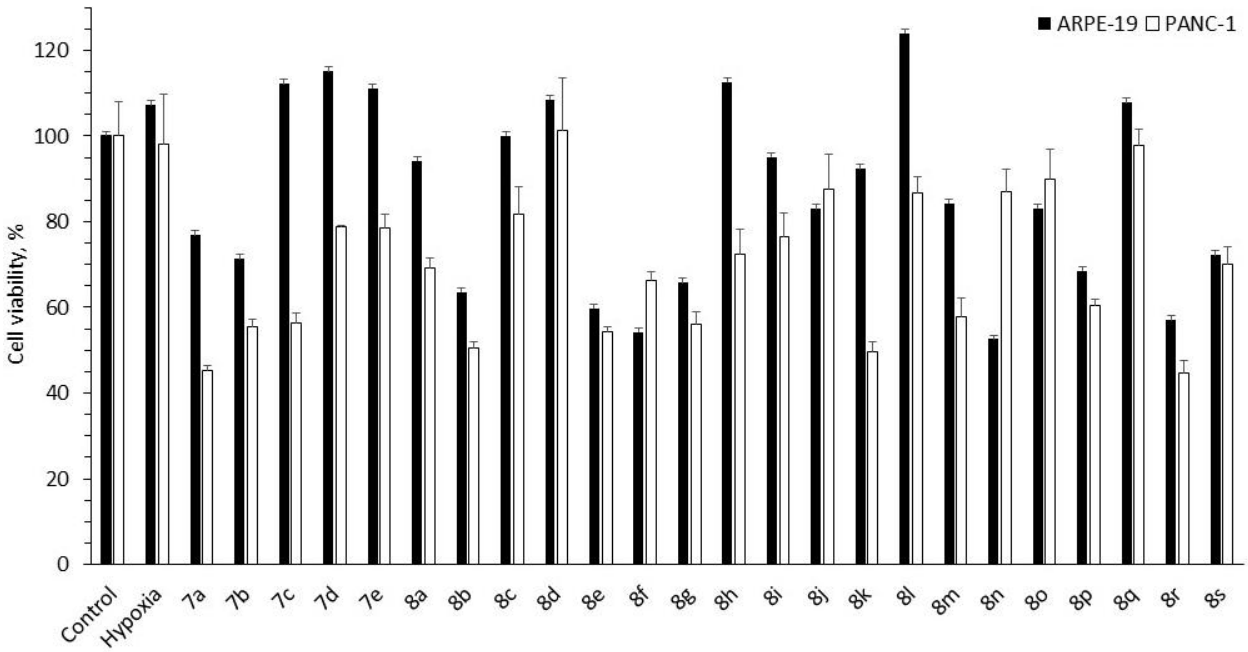

Fig. 4. Cell viability MTT assay results for compounds **7a-e** and **8a-s** (50 μM) against APRE-19 and PANC-1 cell lines (values are expressed as the mean ± SEM of three experiments: (∗) $P < 0.05$ and (∗∗) $P < 0.01$ in comparison to control (0 μM).

Compounds **7a-e** and **8a-s** were screened at 50 μM concentration for their ability to affect the cell culture viability for a non-cancerous human retinal pigment epithelial cell line ARPE-19 [31] as well as pancreas ductal adenocarcinoma cell line PANC-1 [32]. The initial testing was performed relative to control (0 μM of the test compounds) under chemically induced ($CoCl_2$) hypoxia [33]. As it is evident from the screening results presented in Fig. 4, cobalt(II) chloride itself did not affect the number of cells in the culture. However, a number of compounds

(particularly, seven compounds **7a**, **7c-e**, **8h**, **8k** and **8l**) proved to be >30% more cytotoxic towards PANC-1 vs. ARPE-19 cell line and were thus perceived as leads worthy further characterization.

These seven frontrunner compounds were tested in the MTT cell viability assay at three different concentrations (30 μM, 100 μM and 300 μM) against normal (ARPE-19) as well as two cancer cell lines (PANC-1 and also melanoma SK-MEL-2 [34] cell line), this time grown under normoxic as well as chemical induced hypoxic conditions. The antiproliferative profiles displayed by compounds **7a**, **7c-e**, **8h**, **8k** and **8l** under this testing scheme are shown in Fig. 5.

Compound **7a** displayed a mild cytotoxicity against ARPE-19 cell line and a roughly similar effect *vs.* PANC-2 cell line (with slightly higher sensitivity under normoxic conditions); the melanoma cell were markedly affected by 300 μM concentrations of **7a** under either normoxia or hypoxia. Compound **7c** proved to be somewhat toxic to normal cells on increasing concentrations. However, at 30 μM, this compound appeared selectively cytotoxic (both under normoxic and hypoxic conditions) to SK-MEL-2 cells *vs.* ARPE-19 and even PANC-1 cells, though with no dose dependency. Compound **7d**, reassuringly, did noticeably affect neither normal nor SK-MEL-2 cells but displayed an obvious and dose-dependent effect on PANC-1 cell line under both normoxic and hypoxic conditions. Compound **7e** was also dose-dependently cytotoxic against PANC-1 cells (at normoxic and, even more so, hypoxic conditions) but not SK-MEL-2 cells. It is considered rather promising, despite some cytotoxicity observed *vs.* ARPE-19 cells. Compounds **8h** and **8l** did not display particularly interesting profiles, considering the absence of selectivity between cells lines at 30 μM and the obvious cytotoxicity to normal cell at higher concentrations. However, compound **8k**, similarly to **7e**, was selectively toxic to PANC-1 cells (with no particular dose dependency) and showed a cleaner profile agains normal (ARPE-19) cells.

Altogether, from these more comprehensive experiments, it can be concluded that compound **7c** can be viewed as a promising cytocoxic agent for melanoma cells (under either hypoxic or normoxic conditions) while compound **8k** was selectively cytotoxic to pancreatic cancer cell under hypoxic conditions. It is noteworthy that both agents can be considered roughly isosteric to each other.

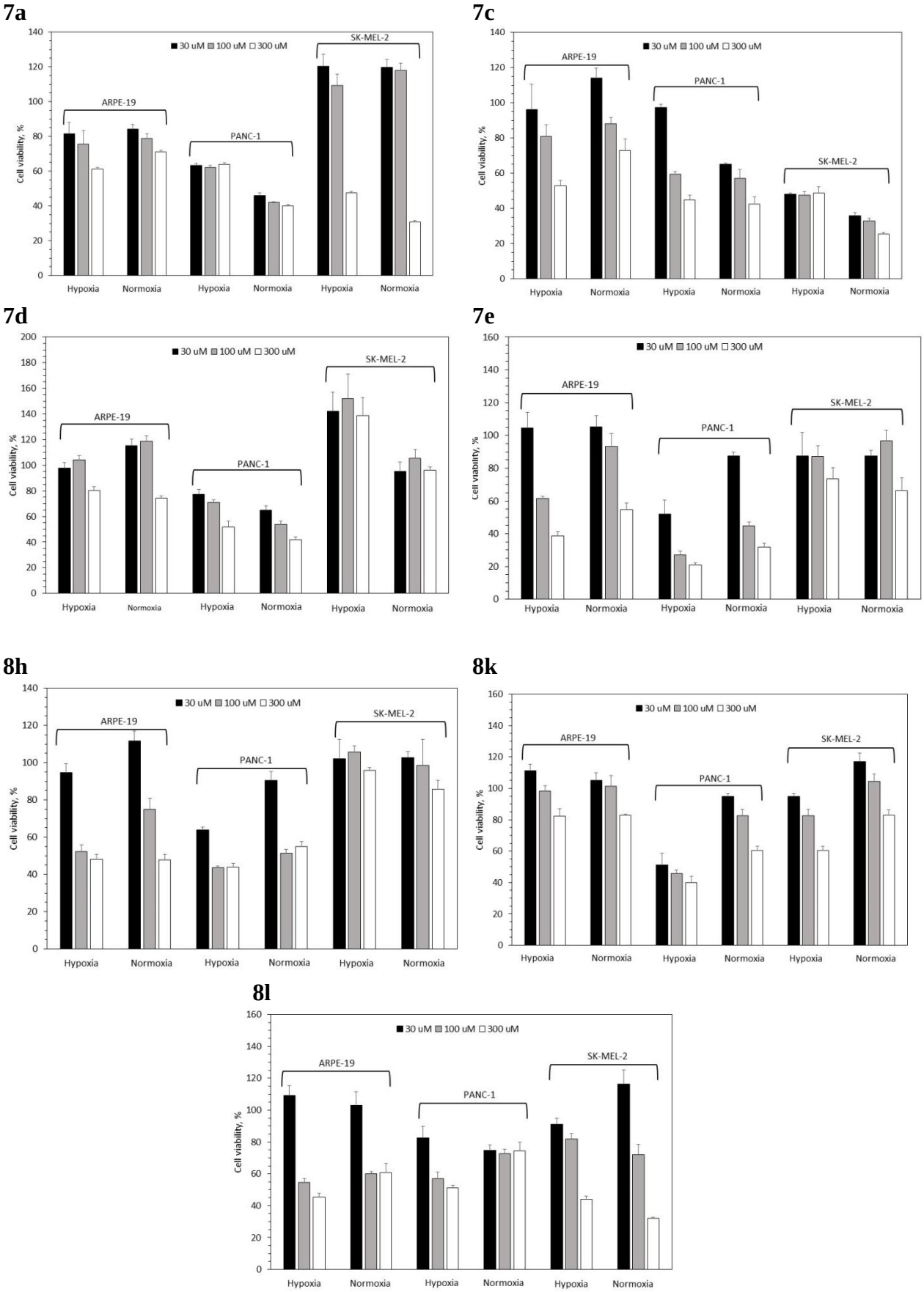

Fig. 5. Cell viability MTT assay results for compounds **7a**, **7c-e**, **8h**, **8k** and **8l** (30 μM, 100 μM and 300 μM) against APRE-19, PANC-1 and MEL cell lines (values are expressed as the mean ± SEM of three experiments: (∗) $P < 0.05$ and (∗∗) $P < 0.01$ in comparison to control (0 μM, not shown).

2.4. Docking studies

The sulfonamide derivatives showing the most interesting SAR were subjected to molecular modeling, including a robust docking procedure followed by energy minimization in explicit water environment (see Experimental section for details), with the aim of predicting their possible binding modes into *h*CAs and thus better rationalizing the observed SAR trends. The obvious detrimental effect, with respect to *h*CA II inhibition, of the methoxy substituent in the phenylene linker present in compounds **8m-p** was analyzed by evaluating the binding disposition of derivatives **8e** and **8n** into the catalytic site of *h*CA II, since these two compounds showed a difference in *h*CA II inhibitory potency corresponding to nearly three orders of magnitude. As shown in Fig. 6A, the subnanomolar inhibitor **8e** coordinates the prosthetic zinc ion of the enzyme through the sulfonamide group, which also forms two H-bonds with the backbone nitrogen and the side chain of T198. The phenylene linker forms hydrophobic interactions with V121, L140 and L197, showing also van der Waals contacts with H94 and Q92, while the oxadiazole ring forms an additional H-bond with the amide group of Q92. Finally, the 4-cyanophenyl group of the ligand shows a π-π stacking with F130 and further lipophilic interactions with I91 and N67. In contrast, the methoxy derivative **8n**, which inhibited *h*CA II with much lower potency, shows a very different binding mode, where the methoxyl group is placed among Q92, V121 and F130, while the 5-aryloxadiazole moiety of the ligand is shifted into a side hydrophobic pocket constituted by F130, V134, L197 and P201 (Fig. 6B). By assuming this disposition, the oxadiazole ring of compound **8n** cannot form the H-bond with Q92. Moreover, the ligand shows reduced lipophilic contacts, thus also losing the π-π stacking interaction with F130. The difference in the pattern of ligand-protein interactions predicted for the two compounds could justify their experimental activities. Interestingly, the same considerations seem to be valid also for their activity against *h*CA IX. In fact, the binding modes calculated for the two analogs **8e** and **8n** within *h*CA IX (Fig. S1) were found to be comparable to those predicted for *h*CA II, in agreement with the comparable potency of the two ligands against *h*CA II and *h*CA IX, as well as with the similar drop of activity of **8n** against *h*CA IX with respect to **8e**.

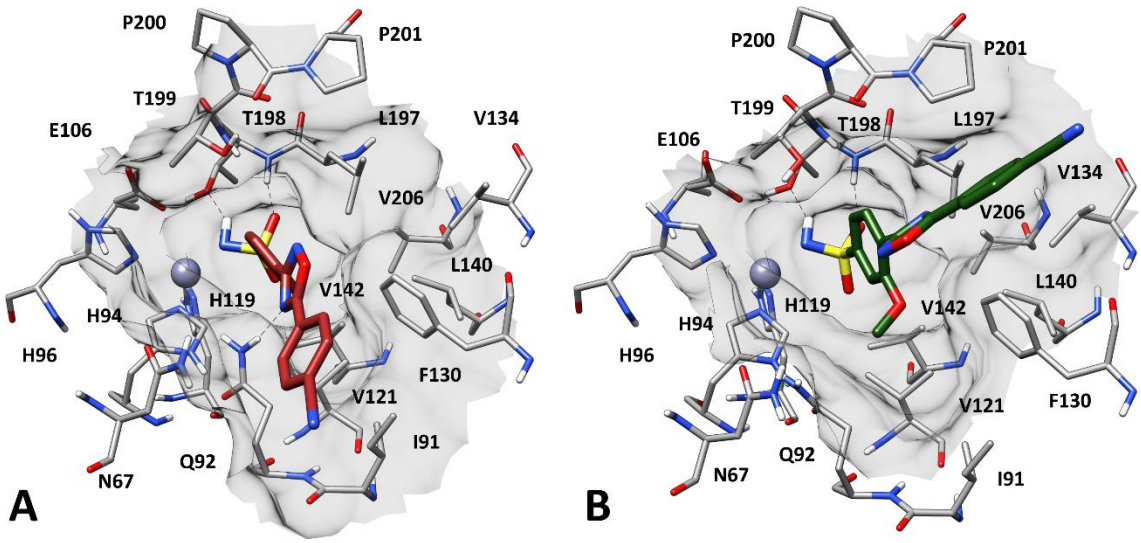

Fig. 6. Predicted binding mode of **8e** (A) and **8n** (B) into *h*CA II. Ligand-protein H-bonds are shown as black dashed lines, the protein surface in the proximity of the ligands is shown in grey.

Compound **8f** and its "scaffold-hopping" counterpart previously reported as compound **6{20}** [23] were analyzed in terms of interactions with both *h*CA II and *h*CA IX. Unsurprisingly, the binding mode into *h*CA II obtained for the two ligands was very similar to that predicted for their structural analogue **8e** (Figure 6A), as both **8f** and **6{20}** showed the same network of interactions among the zinc ion, T198 and their sulfonamide group, the H-bond between the oxadiazole ring and Q92, as well a similar pattern of hydrophobic interactions including a π-π stacking between the pyridine group and F130 (Fig. S2). However, in their putative binding mode within *h*CA IX (Fig. 7) the two compounds showed a different orientation of the pyrid-2-yl 1,2,4-oxadiazole moiety, which was 180° rotated with respect to the disposition into *h*CA II. This orientation was probably adopted to maximize the lipophilic interactions with the hydrophobic wall of *h*CA IX catalytic pocket formed by L223, V262 and L266, which is more flat compared to *h*CA II due to the presence of V262 in place of the non-conserved F130 of *h*CA II. Interestingly, compound **6{20}** shows an H-bond with Q224 of *h*CA IX (homolog of Q92 in *h*CA II), but this interaction is formed through the endocyclic oxygen of its oxadiazole ring (Fig. 7A) and should be thus weaker than that formed through the endocyclic nitrogen. This feature is in agreement with the reduced activity of **6{20}** against *h*CA IX, although it is not sufficient to fully justify the selectivity of **6{20}** toward *h*CA II. In contrast, the heteroatom swap introduced in the oxadiazole ring of **8f** allows this latter ligand to form an H-bond with Q224 of *h*CA IX (Fig. 7B) as strong as that predicted with Q92 in *h*CA II and to retain a comparable inhibitory potency against the two *h*CA isoforms.

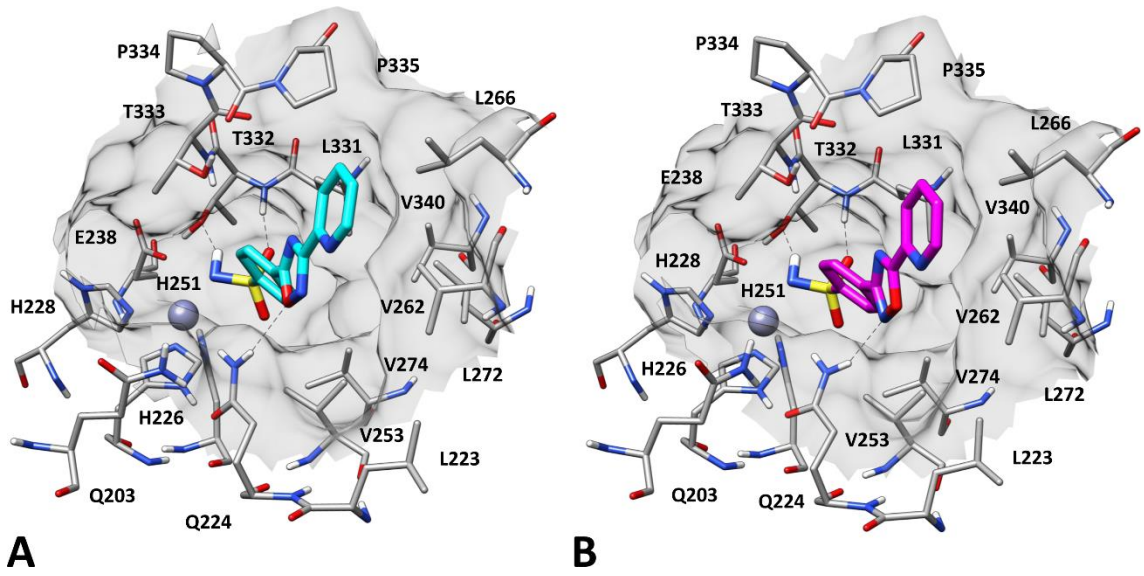

Fig. 7. Predicted binding mode of **6{20}** (A) and **8f** (B) into *h*CA IX. Ligand-protein H-bonds are shown as black dashed lines, the protein surface in the proximity of the ligands is shown in grey.

Finally, perhaps the most interesting inhibitor **7c**, which showed a double-digit picomolar potency against *h*CA IX and a promising antiproliferative activity in melanoma cells, was studied to evaluate its binding mode into *h*CA IX and *h*CA II, together with the phenyl analogue **8k** that showed a selective cytotoxic activity against hypoxic pancreatic cancer cells. As shown in Fig. 8A, the sulfonamide group of **7c** acts as zinc binding group and forms the two H-bonds with T332 as observed for **6{20}** and **8f** (Fig. 7). The cyclopropyl-substituted 1,2,4-oxadiazole portion of the ligand forms multiple hydrophobic interactions with L223, Q224, V253, L272, L274 and shows an H-bond with the amide group of Q224. Finally, the 3,5-thienylene moiety of **7c**, which forms strong lipophilic contacts with L331, is able to establish a fourth H-bond with the hydroxyl group of T333 that contributes to anchor the inhibitor to the catalytic core of the enzyme. On the contrary, compound **8k** was predicted to assume a binding mode with the *m*-phenylene group sandwiched between the side chains of T333 and Q224. In this disposition, the ligand is only able to form the two H-bonds with T322 with its sulfonamide group and hydrophobic interactions with V253, V262, L272, L266, L331 and P335 through the cyclopropyl-substituted 1,2,4-oxadiazole moiety. The two additional H-bonds and the wider lipophilic interactions formed by **7c** with respect to **8k** could be at the basis of the dramatic increase in *h*CA IX inhibitory potency of the thiophene compound compared to its benzene analogue. The predicted binding mode of **7c** and **8k** into *h*CA II were however considerably similar for the two derivatives, in agreement with the much smaller gap of *h*CA II inhibitory activity observed for the two compounds. In fact, both ligands placed their cyclopropyloxadiazole moiety between the side chains of Q92 and F130, forming strong π-π

interactions with both residues and lipophilic interactions with I91 and V121 (Fig. S3). This binding orientation determined the loss of the H-bond formed by the 1,2,4-oxadiazole ring of **7c** with Q224, consistent with the lower activity of the ligand against *h*CA II compared to *h*CA IX. Nevertheless, the compound was still able to form an H-bond with T333 through the thiophene ring (similarly to the interaction with T199 in *h*CA IX) justifying its higher *h*CA II inhibitory potency with respect to **8k**, which could still form only the two H-bonds with T332 through its sulfonamide group.

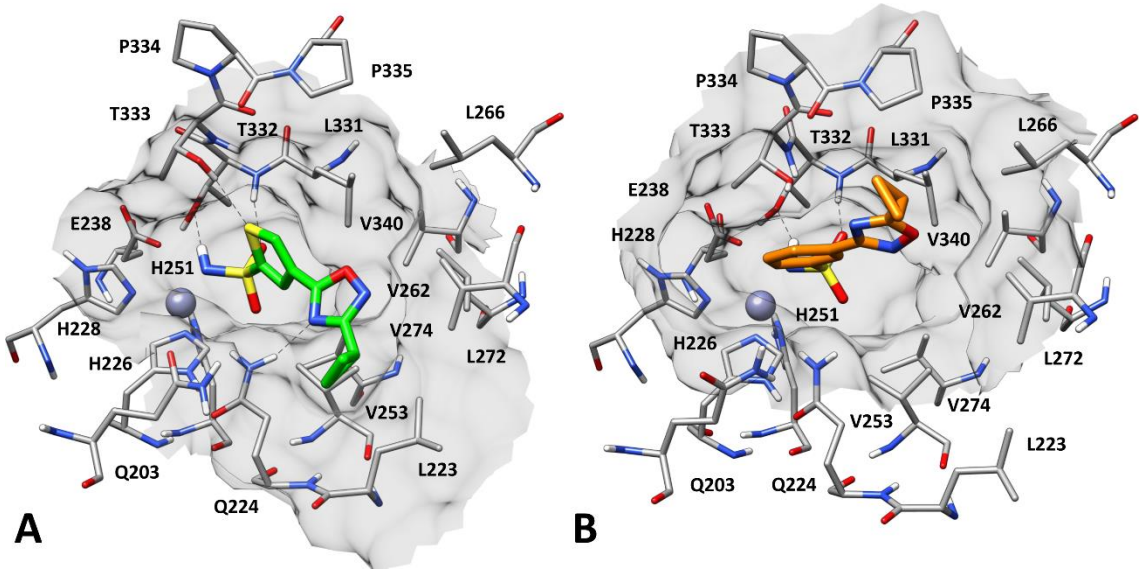

Fig. 8. Predicted binding mode of **7c** (A) and **8k** (B) into *h*CA IX. Ligand-protein H-bonds are shown as black dashed lines, the protein surface in the proximity of the ligands is shown in grey.

3. Conclusion

We have presented the results of comprehensive characterization of subnanomolar *h*CA IX inhibitors belonging to 1,2,4-oxadiazole primary sulfonamide series. Biochemical profiling revealed several interesting SAR trends subsequently rationalized by molecular modeling. Comparative testing for cytotoxicity against normal and cancer cell lines under chemically induced hypoxia conditions (rendering the catalytic activity of *h*CA IX and *h*CA XII crucial for cancer cell survival and its inhibition – a valid approach to killing such cells) delivered several candidates that were selectively toxic to cancer cells. More in-depth testing identified two structurally related promising compounds that displayed selective antiproliferative effects against pancreatic and melanoma cell lines. These results further validate small-molecule inhibition of the membrane-bound *h*CA IX (as well as *h*CA XII) as a therapeutic intervention for cancer.

4. Experimental section

4.1. General experimental

All and reagents and solvents were obtained from commercial sources and used without purification. All reactions implemented in an open flask without any protection from CO_2 and H_2O. Reactions were monitored by analytical thin layer chromatography (TLC) Macherey-Nagel, TLC plates Polygram® Sil G/UV254. Visualization of the developed chromatograms was performed by fluorescence quenching at 254 nm. ^{1}H and ^{13}C NMR spectra were measured on Bruker AVANCE DPX 400 (400 MHz for ^{1}H and 100 MHz for ^{13}C respectively). All chemical shifts (δ) are given in parts per million (ppm) with reference to solvent residues in DMSO-d_6 (2.50 for proton and 39.52 for carbon) and coupling constant (*J)* are reported in hertz (Hz). Multiplicities are abbreviated as follows: s = singlet, d = doublet, t = triplet, q = quartet, m = multiplet, br = broad. Melting points were determined on Electrothermal IA 9300 series Digital Melting Point Apparatus. Mass spectra were recorded on microTOF spectrometers (ESI ionization).

4.2. Synthetic organic chemistry

*4.2.1. Synthesis of 5-sulfamoylthiophene-3-carboxylic acid (**9**)*

Thiophene-3-carboxylic acid (20 mmol) was added portion wise to a stirred and cooled chlorosulfonic acid (1.9 mL, 200 mmol). The resulting mixture was stirred at room temperature for 1 h, then was heated at 60 °C for 3 h and finally poured on crushed ice. The mixture was extracted with dichloromethane (150 mL), dried over anhydrous Na_2SO_4, filtered and concentrated *in vacuo*. The residue was dissolved in MeCN (50 mL) and the solution was treated with 25% aqueous ammonia (100 mmol). The resulting mixture was heated at 50 °C for 1 h, cooled and the volatiles were removed *in vacuo* and 5% hydrochloric acid solution (70 mL) was added. The formed participate was filtered off and dried in air at 50 °C. The yield of 5-sulfamoylthiophene-3-carboxylic acid is 2.90 g (70 %). Beige solid; m.p. 217-220 °C. ^{1}H NMR (400 MHz, DMSO) δ ppm 13.13 (s, 1H), 8.47 (d, J = 1.5 Hz, 1H), 7.84 – 7.77 (m, 3H). ^{13}C NMR (101 MHz, DMSO) δ ppm 163.16, 147.07, 137.58, 134.21, 130.10. HRMS (ESI, *m/z*): calculated for $C_5H_5NO_4S_2$ $[M+Na]^+$ 229.9552; found 229.9556.

4.2.2. General procedure (GP 1): preparation of amidoximes **(10 a-e)** [24]

To a stirred suspension of nitrile (30 mmol) and hydroxylamine hydrochloride (3.13 g, 45 mmol) in EtOH (50 mL) a $NaHCO_3$ (3.78 g, 45 mmol) was added. The reaction mixture was stirred under reflux for 6 h. After the reaction had completed, the reaction mixture was concentrated

under reduced pressure, and the residue was diluted with cold water (80 mL). The resulting precipitate was filtered off, washed with cold water (20 mL) and dried in air at room temperature.

*4.2.3. N'-Hydroxypicolinimidamide (**10a**)* [35]

Yield 3.54 g (86%); White solid; m.p. 117-118 °C. ^{1}H NMR (400 MHz, DMSO) δ ppm 9.90 (s, 1H), 8.57 (d, J = 4.8 Hz, 1H), 7.86 (d, J = 7.9 Hz, 1H), 7.82 (t, J = 8.1 Hz, 1H), 7.40 (t, J = 6.6 Hz, 1H), 5.80 (br.s, 2H).

*4.2.4. N'-Hydroxybenzimidamide (**10b**)* [36]

Yield 3.23 g (79%). White solid; m.p. 76-78 °C. ^{1}H NMR (400 MHz, DMSO) δ ppm 9.60 (s, 1H), 7.73 – 7.62 (m, 2H), 7.42 – 7.32 (m, *3H), 5.78 (br. s, 2H).*

*4.2.5. N'-hydroxy-2-methoxybenzimidamide (**10c**)* [37]

Yield 3.64 g (73%). White solid; m.p. 113-115 °C. ^{1}H NMR (400 MHz, DMSO) δ ppm 9.37 (s, 1H), 7.43 – 7.30 (m, 2H), 7.05 (dd, J = 8.2, 2.2 Hz, 1H), 6.93 (td, J = 7.4, 2.2 Hz, 1H), 5.59 (br.s, 2H), 3.79 (d, J = 2.7 Hz, 3H).

*4.2.6. N'-hydroxy-3-methoxybenzimidamide (**10d**)* [38]

Yield 4.04 g (81%). White solid; m.p. 109-110 °C. ^{1}H NMR (400 MHz, DMSO) δ ppm 9.62 (s, 1H), 7.34 – 7.16 (m, 3H), 6.93 (dt, J = 6.7, 2.6 Hz, 1H), 5.79 (br.s, 2H), 3.76 (s, 3H).

*4.2.7. N'-hydroxycyclopropanecarboximidamide (**10e**)* [36]

Yield 1.56 g (52%). Light brown viscous liquid. ^{1}H NMR (400 MHz, DMSO) δ ppm 8.69 (s, 1H), 5.18 (br.s, 2H), 1.31 (dq, J = 8.4, 5.2 Hz, 1H), 0.71 – 0.49 (m, 4H).

*4.2.8. N'-hydroxy-4-sulfamoylbenzimidamide (**10f**)* [39]

Yield 6.00 g (93%). Beige solid; m.p. 218-219 °C. ^{1}H NMR (400 MHz, DMSO-d_6,) δ ppm 9.86 (s, 1H), 7.82 (m, 4H), 7.37 (s, 2H), 5.93 (br.s, 2H).

*4.2.9. N'-Hydroxythiophene-3-carboximidamide (**10g**)* [27]

Yield 3.5 g (82%). Beige solid; m.p. 85-86 °C. ^{1}H NMR (400 MHz, DMSO-d_6,) δ ppm 9.45 (s, 1H), 7.80 (d, 1H, J = 0.9 Hz), 7.49 (m, 1H), 7.33 (d, J = 5.0 Hz, 1H), 5.76 (br.s, 2H).

4.2.10. N'-hydroxy-3-sulfamoylbenzimidamide (***10h***) [27].

Yield 5.75 g (89%). Beige solid; m.p. 178-179 °C. ^{1}H NMR (400 MHz, DMSO-d_6,) δ ppm 9.81 (s, 1H), 8.17 (t, J = 1.6 Hz, 1H), 7.85 (d, J = 7.9 Hz, 1H), 7.82 (d, J = 8.2 Hz, 1H), 7.58 (t, J = 7.8 Hz, 1H), 7.37 (s, 2H), 5.93 (br.s, 2H).

4.2.11. N'-hydroxy-2-methoxy-4-sulfamoylbenzimidamide (***10h***)

Yield 6.07 g (94%). Beige solid; m.p. 204-206 °C. ^{1}H NMR (400 MHz, DMSO) δ ppm 9.50 (s, 1H), 7.85 (d, J = 2.4 Hz, 1H), 7.79 (dd, J = 8.7, 2.5 Hz, 1H), 7.31 – 7.18 (m, 3H), 5.70 (br.s, 2H), 3.87 (s, 3H). ^{13}C NMR (101 MHz, DMSO) δ ppm 159.9, 150.4, 136.3, 128.4, 128.0, 123.3, 112.3, 56.6. HRMS (ESI, *m/z*): calculated for $C_8H_{11}N_3O_4S$ $[M+H]^+$ 246.0543; found 246.0552.

4.2.12. General procedure (GP 2): preparation of 1,2,4-oxadiazoles via reaction of amidoximes and carboxylic acid [28]

To a solution of carboxylic acid 1 (1.1 mmol) in dry DMSO (1.0 mL) CDI (195 mg, 1.2 mmol) was added. The reaction mixture was stirred at room temperature for 30 min, and then amidoxime **10** (1.0 mmol) was added. The reaction mixture was stirred at room temperature for another 18 h, then to the reaction mixture powdered NaOH (48 mg, 1.2 mmol) was added rapidly. The reaction mixture was stirred at room temperature for 2 h. Then the reaction mixture was diluted with cold water (20 mL). The resulting precipitate was filtered off, washed with cooled water (15 mL) and dried in air at 50 °C.

*4.2.14. 4-(3-(2-Methoxyphenyl)-1,2,4-oxadiazol-5-yl)thiophene-2-sulfonamide (**7b**)*

Yield 229 mg (68%). Beige solid, m.p. 261-263 °C. ^{1}H NMR (400 MHz, DMSO-d_6) δ ppm 8.79 (d, J = 1.4 Hz, 1H), 8.05 (d, J = 1.5 Hz, 1H), 7.93 – 7.87 (m, 3H), 7.61 – 7.56 (m, 1H), 7.25 (d, J = 8.2 Hz, 1H), 7.14 (t, J = 7.5 Hz, 1H), 3.89 (s, 3H). ^{13}C NMR (101 MHz, DMSO-d_6) δ ppm 170.1, 167.2, 158.2, 149.2, 135.6, 133.3, 131.3, 128.4, 124.8, 121.0, 115.4, 112.9, 56.4. HRMS (ESI, *m/z*): calculated for $C_{13}H_{11}N_3O_4S_2$ $[M+H]^+$ 338.0264; found 338.0271.

*4.2.15 4-(3-Cyclopropyl-1,2,4-oxadiazol-5-yl)thiophene-2-sulfonamide (**7c**)*

Yield 203 mg (75%). White solid, m.p. 311-313 °C. ^{1}H NMR (400 MHz, DMSO) δ ppm 8.72 (d, J = 1.6 Hz, 1H), 7.97 (d, J = 1.6 Hz, 1H), 7.90 (s, 2H), 2.19 (m, 1H), 1.15 – 1.09 (m, 2H), 1.00 – 0.95 (m, 2H). ^{13}C NMR (101 MHz, DMSO) δ ppm 173.0, 170.6, 148.8, 135.5, 128.5, 124.8, 8.1, 6.9. HRMS (ESI, *m/z*): calculated for $C_9H_9N_3O_3S_2$ $[M+H]^+$ 272.0158; found 272.0152.

*4.2.16. 4-(3-(Pyridin-2-yl)-1,2,4-oxadiazol-5-yl)thiophene-2-sulfonamide (**7d**)*

Yield 222 mg (72%). Beige solid, m.p. 239-241 °C. ^{1}H NMR (400 MHz, DMSO-d_6) δ ppm 8.87 (s, 1H), 8.79 (d, J = 4.5 Hz, 1H), 8.15 (d, J = 7.7 Hz, 1H), 8.10 (s, 1H), 8.06 (t, J = 7.6 Hz, 1H),

7.97 (s, 2H), 7.64 (t, J = 5.0 Hz, 1H). ^{13}C NMR (101 MHz, DMSO-d_6) δ ppm 171.5, 168.7, 150.8, 149.0, 145.9, 138.2, 136.1, 128.5, 126.7, 124.6, 123.9. HRMS (ESI, *m/z*): calculated for $C_{11}H_8N_4O_3S_2$ $[M+Na]^+$ 330.9930; found 330.9941.

*4.2.17. 4-(3-(3-Methoxyphenyl)-1,2,4-oxadiazol-5-yl)thiophene-2-sulfonamide (**7e**)*

Yield 222 mg (66%). Yellow solid, m.p. 167-169 °C. ^{1}H NMR (400 MHz, DMSO-d_6) δ ppm 8.85 (d, J = 1.5 Hz, 1H), 8.10 (d, J = 1.5 Hz, 1H), 7.95 (s, 2H), 7.66 (d, J = 7.7 Hz, 1H), 7.57 – 7.55 (m, 1H), 7.52 (t, J = 8.0 Hz, 1H), 7.20 (dd, J = 8.3, 2.6 Hz, 1H), 3.86 (s, 3H). ^{13}C NMR (101 MHz, DMSO-d_6) δ ppm 171.3, 168.5, 160.2, 149.0, 135.9, 131.0, 128.6, 127.7, 124.7, 119.9, 118.2, 112.5, 55.8. HRMS (ESI, *m/z*): calculated for $C_{13}H_{11}N_3O_4S_2$ $[M+H]^+$ 338.0264; found 338.0266.

*4.2.18. 4-(5-(Thiophen-3-yl)-1,2,4-oxadiazol-3-yl)benzenesulfonamide (**8b**)*

Yield 157 mg (51%). Beige solid, m.p. 279-281 °C. ^{1}H NMR (400 MHz, DMSO-d_6) δ ppm 8.70 (s, 1H), 8.26 (d, J = 8.4 Hz, 2H), 8.04 (t, J = 6.7 Hz, 2H), 7.89 (dd, J = 5.0, 2.9 Hz, 1H), 7.77 (d, J = 5.1 Hz, 1H), 7.55 (s, 2H). ^{13}C NMR (101 MHz, DMSO-d_6) δ ppm 172.6, 167.7, 147.1, 132.8, 129.9, 129.5, 128.2, 127.1, 126.8, 125.0. HRMS (ESI, *m/z*): calculated for $C_{12}H_9N_3O_3S_2$ $[M+Na]^+$ 329.9978; found 329.9987.

*4.2.19. 4-(5-(Thiophen-2-yl)-1,2,4-oxadiazol-3-yl)benzenesulfonamide (**8h**)*

Yield 215 mg (70%). White solid, m.p. 218-219 °C. ^{1}H NMR (400 MHz, DMSO-d_6) δ ppm 8.25 (d, J = 8.3 Hz, 2H), 8.14 (d, J = 4.6 Hz, 1H), 8.12 (d, J = 3.7 Hz, 1H), 8.03 (d, J = 8.3 Hz, 2H), 7.55 (s, 2H), 7.41 – 7.36 (m, 1H). ^{13}C NMR (101 MHz, DMSO-d_6) δ ppm 172.0, 167.8, 147.2, 134.9, 133.6, 129.8, 129.3, 128.3, 127.1, 124.8. HRMS (ESI, *m/z*): calculated for $C_{12}H_9N_3O_3S_2$ $[M+H]^+$ 308.0158; found 308.0169.

*4.2.20. 4-(5-(Pyridin-2-yl)-1,2,4-oxadiazol-3-yl)benzenesulfonamide (**8f**)*

Yield 239 mg (79%). Beige solid, m.p. 295-297 °C. ^{1}H NMR (400 MHz, DMSO) δ ppm 8.88 (d, J = 4.1 Hz, 1H), 8.37 (d, J = 7.8 Hz, 1H), 8.32 (d, J = 8.5 Hz, 2H), 8.16 (td, J = 7.8, 1.7 Hz, 1H), 8.06 (d, J = 8.5 Hz, 2H), 7.77 (ddd, J = 7.6, 4.8, 1.0 Hz, 1H), 7.57 (s, 2H). ^{13}C NMR (101 MHz, DMSO-d_6) δ ppm 175.2, 168.0, 151.1, 147.2, 143.1, 138.6, 129.4, 128.3, 128.1, 127.1, 125.0. HRMS (ESI, *m/z*): calculated for $C_{13}H_{10}N_4O_3S$ $[M+H]^+$ 303.0546; found 303.0550.

*4.2.21. 3-(5-(Thiophen-3-yl)-1,2,4-oxadiazol-3-yl)benzenesulfonamide (**8l**)*

Yield 193 mg (63%). Beige solid, m.p. 246-248 °C. ^{1}H NMR (400 MHz, DMSO-d_6) δ ppm 8.71 (d, J = 1.6 Hz, 1H), 8.52 (s, 1H), 8.28 (d, J = 7.9 Hz, 1H), 8.05 (d, J = 7.8 Hz, 1H), 7.89 (dd, J = 5.1, 2.9 Hz, 1H), 7.80 (dd, J = 15.8, 6.5 Hz, 2H), 7.57 (s, 2H). ^{13}C NMR (101 MHz, DMSO-d_6) δ

ppm 172.7, 167.7, 145.6, 132.8, 130.7, 130.6, 129.8, 129.0, 127.4, 126.7, 125.0, 124.7. HRMS (ESI, *m/z*): calculated for $C_{12}H_9N_3O_3S_2$ $[M+H]^+$ 308.0158; found 308.0138.

*4.2.22. 3-Methoxy-4-(5-(pyridin-3-yl)-1,2,4-oxadiazol-3-yl)benzenesulfonamide (**8o**)*

Yield 139 mg (42%). Beige solid, m.p. 264-266 °C. ^{1}H NMR (400 MHz, DMSO-d_6) δ ppm 9.33 (d, J = 1.5 Hz, 1H), 8.89 (dd, J = 4.8, 1.5 Hz, 1H), 8.61 – 8.50 (m, 1H), 8.45 (d, J = 2.4 Hz, 1H), 8.02 (dd, J = 8.8, 2.4 Hz, 1H), 7.70 (dd, J = 7.7, 5.2 Hz, 1H), 7.46 (d, J = 8.9 Hz, 1H), 7.41 (s, 2H), 4.00 (s, 3H). ^{13}C NMR (101 MHz, DMSO-d_6) δ ppm 173.3, 166.4, 160.5, 154.1, 148.9, 136.8, 136.1, 131.1, 129.1, 125.0, 120.4, 115.3, 113.3, 57.1. HRMS (ESI, *m/z*): calculated for $C_{14}H_{12}N_4O_4S$ $[M+H]^+$ 333.0652; found 333.0659.

*4.2.23. 3-Methoxy-4-(5-(thiophen-2-yl)-1,2,4-oxadiazol-3-yl)benzenesulfonamide (**8p**)*

Yield 212 mg (63%). Beige solid, m.p. 284-286 °C. ^{1}H NMR (400 MHz, DMSO-d_6) δ ppm 8.40 (d, J = 2.4 Hz, 1H), 8.11 (d, J = 5.0 Hz, 1H), 8.09 (d, J = 3.7 Hz, 1H), 8.01 (dd, J = 8.8, 2.4 Hz, 1H), 7.44 (d, J = 8.9 Hz, 1H), 7.40 (s, 2H), 7.37 (t, J = 4.9 Hz, 1H), 3.99 (s, 3H). ^{13}C NMR (101 MHz, DMSO-d_6) δ ppm 170.6, 166.2, 160.5, 136.8, 134.5, 133.3, 131.0, 129.8, 129.1, 124.9, 115.4, 113.3, 57.1. HRMS (ESI, *m/z*): calculated for $C_{13}H_{11}N_3O_4S_2$ $[M+H]^+$ 338.0264; found 338.0241.

4.2.24. General procedure (GP 3): the synthesis of 1,2,4-oxadiazoles via reaction of amidoximes and carboxylic acid esters [26]

To a solution of amidoxime **10** (1.0 mmol) and ester (1.5 mmol) in DMSO (1.0 mL) powdered NaOH (60 mg, 1.5 mmol) was rapidly added. The reaction mixture was stirred at room temperature for the required time (TLC or precipitation of the product). The reaction mixture was diluted with cold water (20 mL). The resulting precipitate was filtered off, washed with water (15 mL) and dried in air at 50 °C.

*4.2.25. 4-(3-Phenyl-1,2,4-oxadiazol-5-yl)thiophene-2-sulfonamide (**7a**)*

Yield 181 mg (59%). Beige solid, m.p. 295-297 °C. ^{1}H NMR (400 MHz, DMSO-d_6) δ ppm 8.59 (s, 1H), 8.18 (d, J = 6.9 Hz, 2H), 8.02 (s, 1H), 7.88 (s, 2H), 7.75 (t, J = 7.1 Hz, 1H), 7.67 (t, J = 7.5 Hz, 2H). ^{13}C NMR (101 MHz, DMSO-d_6) δ ppm 176.0, 164.6, 148.5, 134.0, 133.2, 130.1, 128.4, 128.2, 127.4, 123.6. HRMS (ESI, *m/z*): calculated for $C_{12}H_9N_3O_3S_2$ $[M+H]^+$ 308.0158; found 308.0155.

*4.2.26. 4-(5-Cyclopropyl-1,2,4-oxadiazol-3-yl)benzenesulfonamide (**8a**)*

Yield 230 mg (87%). White solid, m.p. 235-237 °C. ^{1}H NMR (400 MHz, DMSO-d_6) δ ppm 8.14 (d, J = 8.3 Hz, 2H), 7.98 (d, J = 8.3 Hz, 2H), 7.52 (s, 2H), 2.46 – 2.40 (m, 1H), 1.31 (dd, J = 6.1,

1.8 Hz, 2H), 1.20 (s, 2H). ^{13}C NMR (101 MHz, DMSO-d_6) δ ppm 182.8, 167.1, 146.9, 129.7, 128.1, 127.0, 10.7, 7.8. HRMS (ESI, *m/z*): calculated for $C_{11}H_{11}N_3O_3S$ $[M+Na]^+$ 288.0413; found 288.0414.

*4.2.27. 4-(5-Phenyl-1,2,4-oxadiazol-3-yl)benzenesulfonamide (**8c**)*

Yield 268 mg (89%). White solid, m.p. 286-288 °C. ^{1}H NMR (400 MHz, DMSO-d_6) δ ppm 8.29 (d, J = 8.6 Hz, 2H), 8.21 (d, J = 7.1 Hz, 2H), 8.05 (d, J = 8.6 Hz, 2H), 7.76 (t, J = 7.4 Hz, 1H), 7.68 (t, J = 7.4 Hz, 2H), 7.56 (s, 2H). ^{13}C NMR (101 MHz, DMSO-d_6) δ ppm 176.3, 167.9, 147.1, 134.0, 130.1, 129.5, 128.4, 128.2, 127.1, 123.6. HRMS (ESI, *m/z*): calculated for $C_{14}H_{11}N_3O_3S$ $[M+Na]^+$ 324.0413; found 324.0425.

*4.2.28. 4-(5-(Pyridin-4-yl)-1,2,4-oxadiazol-3-yl)benzenesulfonamide (**8d**)*

Yield 214 mg (71%). White solid, m.p. 245-247 °C. ^{1}H NMR (400 MHz, DMSO-d_6) δ ppm 8.93 (dd, J = 4.4, 1.6 Hz, 2H), 8.30 (d, J = 8.5 Hz, 2H), 8.12 (dd, J = 4.4, 1.6 Hz, 2H), 8.05 (d, J = 8.6 Hz, 2H), 7.49 (s, 2H). ^{13}C NMR (101 MHz, DMSO-d_6) δ ppm 174.8, 168.2, 151.7, 147.4, 130.7, 129.1, 128.3, 127.2, 121.8. HRMS (ESI, *m/z*): calculated for $C_{13}H_{10}N_4O_3S$ $[M+H]^+$ 303.0546; found 303.0548.

*4.2.29. 4-(5-(4-Cyanophenyl)-1,2,4-oxadiazol-3-yl)benzenesulfonamide (**8e**)*

Yield 205 mg (63%). White solid, m.p. 297-299 °C. ^{1}H NMR (400 MHz, DMSO-d_6) δ ppm 8.37 (d, J = 8.6 Hz, 2H), 8.30 (d, J = 8.6 Hz, 2H), 8.15 (d, J = 8.6 Hz, 2H), 8.05 (d, J = 8.5 Hz, 2H), 7.57 (s, 2H). ^{13}C NMR (75 MHz, DMSO-d_6) δ ppm 174.9, 168.1, 147.3, 133.9, 129.2, 128.3, 127.5, 127.1, 118.3, 116.0. HRMS (ESI, *m/z*): calculated for $C_{15}H_{10}N_4O_3S$ $[M+Na]^+$ 349.0366; found 349.0402.

*4.2.30. 4-(5-(3,4-Dichlorophenyl)-1,2,4-oxadiazol-3-yl)benzenesulfonamide (**8g**)*

Yield 203 mg (55%). White solid, m.p. 208-210 °C. ^{1}H NMR (400 MHz, DMSO-d_6) δ ppm 8.40 (d, J = 1.9 Hz, 1H), 8.29 (d, J = 8.3 Hz, 2H), 8.17 (dd, J = 8.4, 1.9 Hz, 1H), 8.04 (d, J = 8.4 Hz, 2H), 7.96 (d, J = 8.4 Hz, 1H), 7.56 (s, 2H). ^{13}C NMR (101 MHz, DMSO-d_6) δ ppm 174.4, 168.0, 147.3, 136.9, 133.0, 132.5, 130.1, 129.2, 128.5, 128.3, 127.1, 124.1. HRMS (ESI, *m/z*): calculated for $C_{14}H_9Cl_2N_3O_3S$ $[M+H]^+$ 369.9814; found 369.9821.

*4.2.31. 4-(5-Methyl-1,2,4-oxadiazol-3-yl)benzenesulfonamide (**8i**)*

Yield 206 mg (86%). White solid, m.p. 214-215 °C. ^{1}H NMR (400 MHz, DMSO-d_6) δ ppm 8.18 (d, J = 8.5 Hz, 2H), 8.00 (d, J = 8.5 Hz, 2H), 7.53 (s, 2H), 2.68 (s, 3H). ^{13}C NMR (101 MHz, DMSO-d_6) δ ppm 178.4, 167.2, 146.9, 129.7, 128.0, 127.1, 12.5. HRMS (ESI, *m/z*): calculated for $C_9H_9N_3O_3S$ $[M+H]^+$ 240.0437; found 240.0433.

*4.2.32. 3-(5-Phenyl-1,2,4-oxadiazol-3-yl)benzenesulfonamide (**8j**)*

Yield 226 mg (75%). White solid, m.p. 267-269 °C. ^{1}H NMR (400 MHz, DMSO-d_6) δ ppm 8.55 (s, 1H), 8.31 (d, J = 7.9 Hz, 1H), 8.22 (d, J = 7.1 Hz, 2H), 8.06 (d, J = 7.9 Hz, 1H), 7.82 (t, J = 7.8 Hz, 1H), 7.76 (t, J = 7.4 Hz, 1H), 7.68 (t, J = 7.4 Hz, 2H), 7.58 (s, 2H). ^{13}C NMR (101 MHz, DMSO-d_6) δ ppm 176.3, 167.9, 145.7, 134.0, 130.8, 130.6, 130.1, 129.1, 128.5, 127.3, 124.7, 123.7. HRMS (ESI, *m/z*): calculated for $C_{14}H_{11}N3O_3S$ $[M+H]^+$ 302.0594; found 302.0601.

*4.2.33. 3-(5-Cyclopropyl-1,2,4-oxadiazol-3-yl)benzenesulfonamide (**8k**)*

Yield 151 mg (57%). Beige solid, m.p. 249-251 °C. ^{1}H NMR (400 MHz, DMSO-d_6) δ ppm 8.40 (s, 1H), 8.17 (d, J = 6.7 Hz, 1H), 8.00 (d, J = 8.2 Hz, 1H), 7.76 (t, J = 7.7 Hz, 1H), 7.53 (s, 2H), 2.47 – 2.40 (m, 1H), 1.36 – 1.27 (m, 2H), 1.24 – 1.18 (m, 2H). ^{13}C NMR (101 MHz, DMSO-d_6) δ ppm 182.8, 167.10, 145.6, 130.6, 130.4, 128.8, 127.4, 124.6, 10.7, 7.7. HRMS (ESI, *m/z*): calculated for $C_{11}H_{11}N_3O_3S$ $[M+H]^+$ 266.0594; found 266.0618.

*4.2.34. 3-Methoxy-4-(5-phenyl-1,2,4-oxadiazol-3-yl)benzenesulfonamide (**8m**)*

Yield 255 mg (77%). Beige solid, m.p. 298-300 °C. ^{1}H NMR (400 MHz, DMSO-d_6) δ ppm 8.45 (d, J = 2.4 Hz, 1H), 8.19 (d, J = 7.0 Hz, 2H), 8.01 (dd, J = 8.8, 2.4 Hz, 1H), 7.75 (t, J = 7.4 Hz, 1H), 7.67 (t, J = 7.4 Hz, 2H), 7.45 (d, J = 8.9 Hz, 1H), 7.40 (s, 2H), 4.00 (s, 3H). ^{13}C NMR (101 MHz, DMSO-d_6) δ ppm 174.9, 166.4, 160.5, 136.8, 133.8, 131.0, 130.1, 129.1, 128.4, 123.7, 115.6, 113.3, 57.1. HRMS (ESI, *m/z*): calculated for $C_{15}H_{13}N_3O_4S$ $[M+Na]^+$ 354.0519; found 354.0521.

*4.2.35. 4-(5-(4-Cyanophenyl)-1,2,4-oxadiazol-3-yl)-3-methoxybenzenesulfonamide (**8n**)*

Yield 192 mg (54%). White solid, m.p. 215-217 °C. ^{1}H NMR (400 MHz, DMSO-d_6) δ ppm 8.45 (d, J = 2.4 Hz, 1H), 8.35 (d, J = 8.7 Hz, 2H), 8.14 (d, J = 8.7 Hz, 2H), 8.02 (dd, J = 8.8, 2.4 Hz, 1H), 7.46 (d, J = 8.9 Hz, 1H), 7.40 (s, 2H), 4.00 (s, 3H). ^{13}C NMR (101 MHz, DMSO-d_6) δ ppm 173.6, 166.6, 160.5, 136.8, 133.9, 131.1, 129.2, 127.6, 118.4, 115.8, 115.2, 113.4, 57.1. HRMS (ESI, *m/z*): calculated for $C_{16}H_{12}N_4O_4S$ $[M+H]^+$ 357.0652; found 357.0635.

*4.2.36. 5-Methyl-3-(thiophen-3-yl)-1,2,4-oxadiazole (**13a**)*

Yield 148 mg (89%). Brown solid, m.p. 153-155 °C. ^{1}H NMR (400 MHz, DMSO) δ ppm 7.87 (dd, J = 5.0, 1.2 Hz, 1H), 7.78 (dd, J = 3.7, 1.2 Hz, 1H), 7.26 (dd, J = 5.0, 3.7 Hz, 1H), 2.65 (s, 3H). ^{13}C NMR (101 MHz, DMSO) δ ppm 177.9, 164.2, 131.0, 130.1, 129.0, 128.05, 12.37. HRMS (ESI, m/z): calculated for C7H6N2OS [M+Na]+ 189.0093; found 189.0099.

*4.2.37. 5-Cyclopropyl-3-(thiophen-3-yl)-1,2,4-oxadiazole **(13b)***

Yield 153 mg (80%). Yellow solid, m.p. 35-37 °C. ^{1}H NMR (400 MHz, DMSO) δ ppm 8.24 – 8.18 (m, 1H), 7.77 – 7.71 (m, 1H), 7.54 (dd, J = 5.1, 1.2 Hz, 1H), 2.37 (dq, J = 8.4, 4.8 Hz, 1H), 1.30 – 1.23 (m, 2H), 1.20 – 1.14 (m, 2H). ^{13}C NMR (101 MHz, DMSO) δ ppm 181.9, 164.6, 128.9, 128.8, 128.1, 126.1, 10.4, 7.6. HRMS (ESI, m/z): calculated for C9H8N2OS [M+Na]+ 215.0250; found 215.0249.

*4.2.38. 5-Phenyl-3-(thiophen-3-yl)-1,2,4-oxadiazole **(13c)***

Yield 207 mg (91%). White solid, m.p. 125-127 °C. ^{1}H NMR (400 MHz, DMSO) δ 8.37 (dd, J = 2.7, 0.9 Hz, 1H), 8.22 – 8.12 (m, 2H), 7.81 (dd, J = 5.0, 3.0 Hz, 1H), 7.73 (t, J = 7.4 Hz, 1H), 7.70 – 7.61 (m, 3H). ^{13}C NMR (101 MHz, DMSO) δ 175.6, 165.4, 133.8, 130.0, 129.3, 129.2, 128.4, 127.9, 126.2, 123.8. HRMS (ESI, *m/z*): calculated for $C_{12}H_8N_2OS$ $[M+Na]^+$ 229.0430; found 229.0433.

*4.2.39. General procedure (GP 4): the synthesis of compounds **8q-s** via reaction sulfochlorination and sulfoamidation*

Oxadiazole **13 a-c** (0.5 mmol) was added portionwise to a stirred and cooled chlorosulfonic acid (0.67 mL, 10 mmol). The resulting mixture was stirred at room temperature for 4 h, and then poured on crushed ice. The mixture was extracted with dichloromethane (10 mL). The solution was washed with 5% aqueous K_2CO_3 (5 mL), dried over anhydrous Na_2SO_4, filtered and flash chromatographed using dichloromethane as eluent and concentrated *in vacuo.* The residue was dissolved in MeCN (5 mL) and the solution was treated with 25% aqueous ammonia (2.5 mmol). The resulting mixture was heated at 50 °C for 1 h, cooled and the volatiles were removed *in vacuo*. The residue was treated with ice-cold water (15 mL) and the mixture was extracted with ethyl acetate (20 mL). The extract was dried over anhydrous Na_2SO_4, filtered and concentrated *in vacuo*. Chromatography on silica gel using 5% methanol in dichloromethane as eluent afforded the desired sulfonamides.

*4.2.40. 4-(5-Methyl-1,2,4-oxadiazol-3-yl)thiophene-2-sulfonamide **(8q)***

Yield 91 mg (74%). White solid, m.p. 288-290 °C. ^{1}H NMR (400 MHz, DMSO-d_6) δ ppm 8.48 (d, J = 1.6 Hz, 1H), 7.93 (d, J = 1.6 Hz, 1H), 7.85 (s, 1H), 2.65 (s, 3H). ^{13}C NMR (101 MHz, DMSO-d_6) δ ppm 178.1, 164.0, 148.5, 132.8, 128.0, 127.5, 12.4. HRMS (ESI, *m/z*): calculated for $C_7H_7N_3O_3S_2$ $[M+Na]^+$ 267.9821; found 267.9805.

*4.2.41. 4-(5-Cyclopropyl-1,2,4-oxadiazol-3-yl)thiophene-2-sulfonamide **(8r)***

Yield 85 mg (63%). White solid, 168-170 °C. ^{1}H NMR (400 MHz, DMSO-d_6) δ ppm 8.44 (d, J = 1.6 Hz, 1H), 7.90 (d, J = 1.6 Hz, 1H), 7.84 (s, 2H), 2.43 – 2.36 (m, 1H), 1.32 – 1.26 (m, 2H), 1.21 – 1.15 (m, 2H). ^{13}C NMR (101 MHz, DMSO-d_6) δ ppm 182.5, 163.9, 148.4, 132.7, 128.1,

127.5, 10.6, 7.7. HRMS (ESI, *m/z*): calculated for $C_9H_9N_3O_3S_2$ $[M+H]^+$ 272.0158; found 272.0163.

4.2.42. 4-(5-Phenyl-1,2,4-oxadiazol-3-yl)thiophene-2-sulfonamide ***(8s)***

Yield 125 mg (82%). Beige solid, m.p. 238-240 °C. ^{1}H NMR (400 MHz, DMSO-d_6) δ ppm 8.59 (s, 1H), 8.18 (d, J = 7.3 Hz, 2H), 8.02 (s, 1H), 7.88 (s, 2H), 7.74 (d, J = 6.8 Hz, 1H), 7.67 (t, J = 7.2 Hz, 2H). ^{13}C NMR (101 MHz, DMSO-d_6) δ ppm 176.0, 164.6, 148.5, 134.0, 133.2, 130.1, 128.4, 128.2, 127.4, 123.6. HRMS (ESI, *m/z*): calculated for $C_{12}H_9N_3O_3S_2$ $[M+H]^+$ 308.0158; found 308.0140.

4.3. Carbonic anhydrase inhibition assay

An Applied Photophysics stopped-flow instrument has been used for assaying the CA catalyzed CO_2 hydration activity [40]. Phenol red (at a concentration of 0.2 mM) has been used as indicator, working at the absorbance maximum of 557 nm, with 20 mM Tris (pH 8.3) as buffer, and 20 mM Na_2SO_4 (for maintaining constant the ionic strength), following the initial rates of the CA-catalyzed CO_2 hydration reaction for a period of 10–100 s. The CO_2 concentrations ranged from 1.7 to 17 mM for the determination of the kinetic parameters and inhibition constants. For each inhibitor at least six traces of the initial 5–10% of the reaction have been used for determining the initial velocity. The uncatalyzed rates were determined in the same manner and subtracted from the total observed rates. Stock solutions of inhibitor (0.1 mM) were prepared in distilled-deionized water and dilutions up to 0.005 nM were done thereafter with the assay buffer. Inhibitor and enzyme solutions were preincubated together for 15 min at room temperature prior to assay, in order to allow for the formation of the E-I complex. The inhibition constants were obtained by non-linear least-squares methods using PRISM 3 and the Cheng-Prusoff equation, as reported earlier, and represent the mean from at least three different determinations. All CA isoforms were recombinant ones obtained in-house [41-44].

4.4. Cell viability assay

Human cell lines were maintained at 37°C in humidified atmosphere containing air and 5% CO_2 as previously described [45]. Retinal pigment epithelial cells ARPE-19 were obtained from American Type Culture Collection (ATCC, Manassas, VA, USA). Human melanoma cell line SK-MEL-2 were obtained from BioloT (Saint Petersburg, Russian Federation). Pancreas ductal adenocarcinoma cells PANC-1 were obtained from Russian collection cell cultures at the RAS Institute of Cytology (Saint Petersburg, Russian Federation). Cell line were grown in Dulbeccos Modified Eagle's Medium-F12 (BioloT) containing 10% (v/v) heat-inactivated fetal calf serum (FCS, HyClone Laboratories, UT, USA), 1% L-glutamine, 1% sodium pyruvate, 50 U/mL

penicillin, and 50 μg/mL streptomycin (BioloT). Cytotoxicity of carbonic anhydrase inhibitors was evaluated using a routine colorimetric method with tetrazolium dye – 3-(4,5-dimethylthiazol-2-yl)-2,5-diphenyltetrazolium bromide (MTT). The cell lines were incubated for 48 h under normoxia and in the presence of the hypoxia-mimicking agent 50 μM $CoCl_2$ with medium containing different concentrations of carbonic anhydrase inhibitors. Following treatment, Dulbeccos Modified Eagle's Medium-F12 (100 μL/ well) and 20 μL of a 2.5 mg/mL MTT solution were added and cells were incubated for 1 h at 37 °C. The used cell density was 5×10^3 cells/200 μL/well in 96-well microtiter plates. After aspiration of the supernatants, the MTT-formazan crystals formed by metabolically active cells were dissolved in dimethyl sulfoxide (100 μL/well) and absorbance was measured at 540 nm and 690 nm in Varioskan LUX™ Multimode Microplate Reader (Thermo Scientific, USA). Values measured at 540 nm were subtracted for background correction at 690 nm, and the data were plotted as a percent of control untreated samples.

4.5. Molecular modeling studies

The crystal structures of *h*CA II (PDB code 2AW1) and *h*CA IX (PDB code 3IAI) were taken from the Protein Data Bank [46]. Molecular docking calculations were performed with AUTODOCK 4.2 [47] using the improved force field [48]. Autodock Tools were used to identify the torsion angles in the ligand, add the solvent model and assign the Kollman atomic charges to the protein, while ligand charges were calculated with the Gasteiger method. A grid spacing of 0.375 Å and a distance-dependent function of the dielectric constant were used for the energetic map calculations. The ligands were subjected to a robust docking procedure already used in virtuals screening and pose prediction studies [49, 50]. Each docked compound was subjected to 200 runs of the AUTODOCK search using the Lamarckian Genetic Algorithm performing 10 000 000 steps of energy evaluation. The number of individuals in the initial population was set to 500 and a maximum of 10 000 000 generations were simulated during each docking run. All other settings were left as their defaults and the best docked conformations were taken into account. The selected docking poses were then refined through energy minimization in explicit water environment [51]. The ligand-protein complexes were minimized employing Amber 16 software [52] with ff14SB force field. The complexes were placed in a rectangular parallelepiped water box, using the TIP3P explicit solvent model for water, and were solvated with a 15 Å water cap. Sodium ions were added as counter ions to neutralize the system. Two minimization stages consisting of 5000 steps of steepest descent followed by conjugate gradient, until a convergence of 0.05 kcal/Å mol, were then performed. In the first one, the protein was kept rigid with a position restraint of 100 kcal/mol·$Å^2$ to uniquely minimize the positions of the water

molecules. In the second stage, the entire system was energy minimized by applying a harmonic potential of 10 kcal/mol·$Å^2$ only to the protein α carbons.

Acknowledgements

This research was supported by the Russian Scientific Fund (project grant 14-50-00069). We are grateful to the Centre for Chemical Analysis and Materials Research of Saint Petersburg State University Research Park for the high-resolution mass-spectrometry data.

A. Supplementary material

Supplementary data associated with this article can be found, in the online version, at http://dx.doi.org/xxx.

References

[1] C. T. Supuran, Structure and function of carbonic anhydrases. Biochem. J. 473 (2016) 2023–2032.

[2] V. Alterio, A. Di Fiore, K. D'Ambrosio, C.T. Supuran, D. De Simone, Multiple Binding Modes of Inhibitors to Carbonic Anhydrases: How to Design Specific Drugs Targeting 15 Different Isoforms?, Chem. Rev. 112 (2012) 4421-4468.

[3] C.T. Supuran, Carbonic anhydrase inhibitors and activators for novel therapeutic applications, Future Med. Chem. 3 (2011) 1165-1180.

[4] C.T. Supuran, C. Capasso, The η-class carbonic anhydrases as drug targets for antimalarial agents, Expert Opin. Ther. Targets. 19 (2015) 551–563.

[5] C.T. Supuran, Diuretics: from classical carbonic anhydrase inhibitors to novel applications of the sulfonamides, Curr. Pharm. Des. 14 (2008) 641−648.

[6] C.T. Supuran, A. Scozzafava, F. Mincione, The development of topically acting carbonic anhydrase inhibitors as antiglaucoma agents, Curr. Pharm. Des. 14 (2008) 649−654.

[7] M. Krasavin, M. Korsakov, Z. Zvonaryova, E. Semyonychev, T. Tuccinardi, S. Kalinin, M. Tanç, C.T. Supuran, Human carbonic anhydrase inhibitory profile of mono- and bis-sulfonamides synthesized via a direct sulfochlorination of 3-and 4-(hetero)arylisoxazol-5-amine scaffolds, Bioorg. Med. Chem. 25 (2017) 1914-1925.

[8] C.T. Supuran, S. Kalinin, M. Tanç, P. Sarnpitak, P. Mujumdar, S.-A. Poulsen, M. Krasavin, Isoform-selective inhibitory profile of 2-imidazoline-substituted benzenesulfonamides against a

panel of human carbonic anhydrases, J. Enzyme Inhib. Med. Chem., 31 (Suppl. 1) (2016) 197-202.

[9] G. La Regina, A. Coluccia, V. Famiglini, S. Pelliccia, L. Monti, D. Vullo, E. Nuti, V. Alterio, G. De Simone, S. M. Monti, P. Pan, S. Parkkila, C.T. Supuran, A. Rossello, R. Silvestri, Discovery of 1,1′-Biphenyl-4-sulfonamides as a New Class of Potent and Selective Carbonic Anhydrase XIV Inhibitors, J. Med. Chem. 58 (2015) 8564-8572.

[10] J. Ivanova, F. Carta, D. Vullo, J. Leitans, A. Kazaks, K. Tars, R. Žalubovskis, C.T. Supuran, N-Substituted and ring opened saccharin derivatives selectively inhibit transmembrane, tumor-associated carbonic anhydrases IX and XII, Bioorg. Med. Chem. 25 (2017) 3583-3589.

[11] F. Carta, D. Vullo, S. M. Osman, Z. AlOthman, C. T. Supuran, Synthesis and Carbonic Anhydrase inhibition of a series of SLC-0111 analogs. Bioorg. Med. Chem. 25 (2017) 2569–2576.

[12] Y. Ozawa, N. H. Sugi, T. Nagasu, T. Owa, T. Watanabe, N. Koyanagi, H. Yoshino, K. Kitoh, K. Yoshimatsu, E7070, a novel sulphonamide agent with potent antitumor activity in vitro and in vivo. Eur. J. Cancer 37 (2001) 2275-2282.

[13] S. Singh, C. L. Lomelino, M. Y. Mboge, S. C. Frost, R. McKenna, Molecules 2018 (23) 1045.

[14] F. Abbate, A. Casini, T. Owa, A. Scozzafava, C. T. Supuran, Carbonic anhydrase inhibitors: E7070, a sulfonamide anticancer agent, potently inhibits cytosolic isozymes I and II, and transmembrane, tumor-associated isozyme IX. Bioorg. Med. Chem. Lett. 14 (2004) 217–223.

[15] L. Schwartz, C. T. Supuran, K. O. Alfarouk, The Warburg effect and the hallmarks of cancer. Anticancer Agents Med. Chem. 17 (2017) 164–170.

[16] C. T. Supuran, Carbonic Anhydrase Inhibition and the Management of Hypoxic Tumors, Metabolites 48 (2017) 48.

[17] T. Yamaoka, M. Ohba, T. Ohmori, Molecular-Targeted Therapies for Epidermal Growth Factor Receptor and Its Resistance Mechanisms. Int. J. Mol. Sci. 18 (2017) E2420.

[18] A. Nocentini, C. T. Supuran, Carbonic anhydrase inhibitors as antitumor/antimetastatic agents: a patent review (2008-2018). Expert Opin. Ther. Pat. 28 (2018) 729-740.

[19] C.T. Supuran, How many carbonic anhydrase inhibition mechanisms exist?, J. Enzyme Inhib. Med. Chem. 31 (2016) 345–360.

[20] P.A. Boriack-Sjodin, S. Zeitlin, H.-H. Chen, L. Crenshaw, S. Gross, A. Dantanarayana, P. Delgado, J.A. May, T. Dean, D.W. Christianson, Structural analysis of inhibitor binding to human carbonic anhydrase II, Protein Sci. 7 (1998) 2483-2489.

[21] M. Krasavin, M. Korsakov, M. Dorogov, T. Tuccinardi, N. Dedeoglu, C.T. Supuran, Probing the 'bipolar nature of the carbonic anhydrase active site: Aromatic sulfonamides containing 1,3-oxazol-5-yl moiety as picomolar inhibitors of cytosolic CA I and CA II isoforms, Eur. J. Med. Chem. 101 (2015) 334-347.

[22] M. Krasavin, M. Korsakov, O. Ronzhina, T. Tuccinardi, S. Kalinin, M. Tanç, C. T. Supuran, Primary mono- and bis-sulfonamides obtained via regiospecific sulfochlorination of N-arylpyrazoles: inhibition profile against a panel of human carbonic anhydrases. J. Enz. Inhib. Med. Chem. 2017, 32, 920-934.

[23] M. Krasavin, A. Shetnev, T. Sharonova, S. Baykov, T. Tuccinardi, K. Kalinin, A. Angeli, C. T. Supuran, Heterocyclic Periphery in the Design of Carbonic Anhydrase Inhibitors: 1,2,4-Oxadiazol-5-yl Benzenesulfonamides as Potent and Selective Inhibitors of Cytosolic hCA II and Membrane-Bound hCA IX Isoforms. Bioorg. Chem. 2018, 76, 88-97.

[24] R. M. Srivastava, M. C. Pereira, W. W. M. Faustino, K. Coutinho, J. V. dos Anjos, S. J. de Melo, Synthesis, mechanism of formation, and molecular orbital calculations of arylamidoximes. Monatsh. Chem.140 (2009) 1319–1324.

[25] S. Baykov, T. Sharonova, A. Osipyan, S. Rozhkov, A. Shetnev, A. Smirnov, A Convenient and Mild Method for 1,2,4-Oxadiazole Preparation: Cyclodehydration of O-Acylamidoximes in the Superbase System MOH/DMSO. Tetrahedron Lett. 57 (2016) 2898-2900.

[26] S. Baykov, T. Sharonova, A. Shetnev, S. Rozhkov, S. Kalinin, A. V. Smirnov, The first one-pot ambient-temperature synthesis of 1,2,4-oxadiazoles from amidoximes and carboxylic acid esters. Tetrahedron 73 (2017) 945-951.

[27] M. Tarasenko, N. Duderin, T. Sharonova, S. Baykov, A. Shetnev, A. Smirnov, Room-temperature synthesis of pharmaceutically important carboxylic acids bearing the 1,2,4-oxadiazole moiety. Tetrahedron Lett. 58 (2017) 3672-3677.

[28] T. Sharonova, V. Pankrat'eva, P. Savko, S. Baykov, A. Shetnev, Facile Room-Temperature Assembly of the 1,2,4-Oxadiazole Core from Readily Available Amidoximes and Carboxylic Acids. Tetrahedron Lett. 59 (2018) 2824-2827.

[29] Y. Chi, K. Gao, H. Zhang, M. Takeda, J. Yao, Suppression of cell membrane permeability by suramin: involvement of its inhibitory actions on connexin 43 hemichannels. Br. J. Pharmacol. 171 (2014) 3448-3462.

[30] A. Grandane, M. Tanc, L. Di Cesare Mannelli, F. Carta, C. Ghelardini, R. Žalubovskis, C. T. Supuran, Substituted sulfocoumarins are selective carbonic anhdydrase IX and XII inhibitors with significant cytotoxicity against colorectal cancer cells. J Med Chem. 58 (2015) 3975-3983.

[31] K. C. Dunn, A. E. Aotaki-Keen, F. R. Putkey, L. M. Hjelmeland, ARPE-19, a human retinal pigment epithelial cell line with differentiated properties. Exp Eye Res. 62 (1996) 155-169.

[32] G. Rui, H. C. Silva, L. Carvalho, M. F. Botelho, A. Mota-Pinto, PaCa-2 and PANC-1 – pancreas ductal adenocarcinoma cell lines with neuroendocrine differentiation and somatostatin receptors. Sci Rep. 6 (2016) 21648.

[33] M. S. Al Okail, Cobalt chloride, a chemical inducer of hypoxia-inducible factor-1a in U251 human glioblastoma cell line. J. Saudi Chem. Soc. 14 (2010) 197-201.

[34] A. Caunii, C. Oprean, M. Cristea, A. Ivan, C. Danciu, C. Tatu, V. Paunescu, D. Marti, G. Tzanakakis, D. A. Spandidos, A. Tsatsakis, R. Susan, C. Soica, S. Avram, C. Dehelean, Effects of ursolic and oleanolic on SK-MEL-2 melanoma cells: In vitro and in vivo assays. Int. J. Oncol. 51 (2017) 1651–1660.

[35] S. Borg, K. Luthman, F. Nyberg, L. Terenius, U. Hacksell. 1,2,4-Oxadiazole derivatives of phenylalanine: potential inhibitors of substance P endopeptidase. Eur. J. Med. Chem. 28 (1993) 801–810.

[36] J. K. Augustine, V. Akabote, S. G. Hegde, P. Alagarsamy. PTSA−$ZnCl_2$: An Efficient Catalyst for the Synthesis of 1,2,4-Oxadiazoles from Amidoximes and Organic Nitriles. J. Org. Chem. 74 (2009) 5640–5643.

[37] A. Vörös, Z. Baán, P. Mizsey, Z. Finta. Formation of Aromatic Amidoximes with Hydroxylamine using Microreactor Technology. Org. Process Res. Dev. 16 (2012) 1717–1726.

[38] C.-C Lin, T.-H. Hsieh, P.-Y. Liao, Z.-Y. Liao, C.-W. Chang, Y.-C. Shih, T.-C. Chien. Practical Synthesis of N-Substituted Cyanamides via Tiemann Rearrangement of Amidoximes. Org. Let. 16 (2014) 892–895.

[39] Z. Luo, A. J. Rosenberg, H. Liu, J. Han, Z. Tu. Syntheses and in vitro evaluation of new S1PR1 compounds and initial evaluation of a lead F-18 radiotracer in rodents. Eur. J. Med. Chem. 150 (2018) 796–808.

[40] R.G. Khalifah, The carbon dioxide hydration activity of carbonic anhydrase I. Stop-flow kinetic studies on the native human isoenzymes B and C, J. Biol. Chem. 246 (1971) 2561-2573.

[41] A. Maresca, F. Carta, D. Vullo, C.T. Supuran, Dithiocarbamates strongly inhibit the β-class carbonic anhydrases from Mycobacterium tuberculosis, J. Enzyme Inhib. Med. Chem. 28 (2013) 407–411.

[42] D. Ekinci, N.I. Kurbanoglu, E. Salamci, M. Senturk, C.T. Supuran, Carbonic anhydrase inhibitors: inhibition of human and bovine isoenzymes by benzenesulphonamides, cyclitols and phenolic compounds, J. Enzyme Inhib. Med. Chem. 27 (2012) 845–848.

[43] D. Ekinci, L. Karagoz, D. Ekinci, M. Senturk, C.T. Supuran, Carbonic anhydrase inhibitors: in vitro inhibition of α isoforms (*h*CA I, *h*CA II, *b*CA III, *h*CA IV) by flavonoids, J. Enzyme Inhib. Med. Chem. 28 (2013) 283–288.

[44] C. Alp, A. Maresca, N.A. Alp, M.S. Gültekin, D. Ekinci, A. Scozzafava C.T. Supuran, Secondary/tertiary benzenesulfonamides with inhibitory action against the cytosolic human carbonic anhydrase isoforms I and II, J. Enzyme Inhib. Med. Chem. 28 (2013) 294–298.

[45] A. V. Hubina, A. A. Pogodaev, V. V. Sharoyko, E. G. Vlakh, T. B. Tennikova, Self-assembled spin-labeled nanoparticles based on poly(amino acids). React. Funct. Polym. 100 (2016) 173-180.

[46] H.M. Berman, T. Battistuz, T.N. Bhat, W.F. Bluhm, P.E. Bourne, K. Burkhardt, Z. Feng, G.L. Gilliland, L. Iype, S. Jain, P. Fagan, J. Marvin, D. Padilla, V. Ravichandran, B. Schneider, N. Thanki, H. Weissig, J.D. Westbrook, C. Zardecki, The protein data bank, Acta Crystallogr. D: Biol. Crystallogr. 2002, 58, 899–907.

[47] G.M. Morris, R. Huey, W. Lindstrom, M.F. Sanner, R.K. Belew, D.S. Goodsell, A.J. Olson, AutoDock4 and AutoDockTools4: Automated docking with selective receptor flexibility, J. Comput. Chem. 2009, 30, 2785–2791.

[48] D. Santos-Martins, S. Forli, M.J. Ramos, A.J. Olson, AutoDock4(Zn): an improved AutoDock force field for small-molecule docking to zinc metalloproteins, J. Chem. Inf. Model. 2014, 54, 2371–2379.

[49] G. Poli, A. Gelain, F. Porta, A. Asai, A. Martinelli, T. Tuccinardi T. Identification of a new STAT3 dimerization inhibitor through a pharmacophore-based virtual screening approach. J. Enzyme. Inhib. Med. Chem. 2016, 31, 1011-1017.

[50] F. Dal Piaz, M.B. Vera Saltos, S. Franceschelli, G. Forte, S. Marzocco, T. Tuccinardi, G. Poli, S. Nejad Ebrahimi, M. Hamburger, N. De Tommasi, A. Braca A. Drug Affinity Responsive Target Stability (DARTS) Identifies Laurifolioside as a New Clathrin Heavy Chain Modulator. J. Nat. Prod. 2016, 79, 2681-2692.

[51] M. Aghazadeh Tabrizi, P.G. Baraldi, E. Ruggiero, G. Saponaro, S. Baraldi, G. Poli, T. Tuccinardi, A. Ravani, F. Vincenzi, P.A. Borea, K. Varani. Synthesis and structure activity relationship investigation of triazolo[1,5-a]pyrimidines as CB2 cannabinoid receptor inverse agonists. Eur. J. Med. Chem. 2016, 113, 11-27.

[52] D.A. Case, J.T. Berryman, R.M. Betz, D.S. Cerutti, Darden, R.E. Duke, T.J. Giese, H. Gohlke, A.W. Goetz, N. Homeyer, S. Izadi, P. Janowski, J. Kaus, A. Kovalenko, T.S. Lee, S. LeGrand, P. Li, T. Luchko, R. Luo, B. Madej, K.M. Merz, G. Monard, P. Needham, H. Nguyen, H.T. Nguyen, I. Omelyan, A. Onufriev, D.R. Roe, A. Roitberg, R. Salomon-Ferrer, C.L. Simmerling, W. Smith, J. Swails, R.C. Walker, J. Wang, R.M. Wolf, X. Wu, D.M. York, P.A. Kollman, AMBER, Version 16, University of California, San Francisco, CA.